Profiling of cellular immune responses to *Mycoplasma pulmonis* infection in C57BL/6 and DBA/2 mice

（C57BL/6 マウスと DBA/2 マウスにおける *Mycoplasma pulmonis* 感染に対する細胞免疫反応のプロファイリング）

Tussapon Boonyarattanasoonthorn

Laboratory of Laboratory Animal Science and Medicine

Department of Applied Veterinary Science

Graduate School of Veterinary Medicine

Hokkaido University

Japan

ABBREVIATIONS

ANOVA	Analysis of variance
B6	C57BL/6 (C57BL/6NCrSlc)
BALF	Bronchoalveolar lavage fluid
b.w.	Body weight
CFU	Colony-forming unit
Chr	Chromosome
cM	Centimorgan
D2	DBA/2 (DBA/2CrSlc)
d.p.i.	Days post infection
EDTA	Ethylenediaminetetraacetic acid
H&E	Hematoxylin and eosin
IFN- γ	Interferon-gamma
IL	Interleukin
LCs	Lymphoid clusters
LOD	Logarithm of the odds
LRS	Likelihood ratio statistic
Mbp	Mega base pairs
MFTs	Mediastinal fat tissues
MGI	Mouse genome informatics
M. pulmonis	*Mycoplasma pulmonis*
PBS	Phosphate-buffered saline

PCR	Polymerase chain reaction
QTL	Quantitative trait locus
SE	Standard error
SPF	Specific pathogen-free
TNF-α	Tumor necrosis factor-alpha

TABLE OF CONTENTS

CHAPTER 2

QTL analysis of resistance/susceptibility to the *Mycoplasma pulmonis* infection in the mouse ····· 35

LIST OF TABLES

LIST OF FIGURES

PREFACE

Mycoplasma infection occurs worldwide and affects mainly in children to young adults and many species of animals. It is spread by close personal contact and has a long incubation period. The infection affects the upper and lower respiratory tracts. Cough, fever, and headache may persist for several weeks. Until now, there is no certified vaccine for mycoplasma infection. Treatment with erythromycin or tetracyclines is effective in reducing symptoms.

Mycoplasmas are spherical to filamentous cells with no cell-walls and presumably evolved by degenerative evolution from Gram-positive bacteria. These bacteria are the smallest self-replicating organisms with the smallest genomes (a total of about 500 to 1,000 genes). Mycoplasmas are nutritionally very exacting. Most of them require cholesterol, a unique property among prokaryotes. Mycoplasmas have surface antigens such as membrane proteins, lipoproteins, glycolipids, and lipoglycans. Some of the membrane proteins undergo spontaneous antigenic variation (39).

Certain *Mycoplasma* species can either activate or suppress host immune systems, and they may use these activities to evade host immune responses. For example, some mycoplasmas can inhibit or stimulate the proliferation of normal lymphocyte subsets, induce B-cell differentiation and trigger the secretion of cytokines, including interleukin (IL)-1, IL-2, IL-4, IL-6, tumor necrosis factor (TNF)-α, interferons, and granulocyte macrophage-colony stimulating factor (GM-CSF) from B-cells as well as other cell types. Moreover, it was also found that *M. fermentans*-derived lipids can interfere with the interferon (IFN)-γ-dependent expression of MHC class II molecules on macrophages. This suppression results in impaired antigen presentation to helper T-cells in an experimental animal model. In addition, mycoplasmas are

able to secret soluble factors that can stimulate proliferation or inhibit the growth and differentiation of immune competent cells. *Mycoplasma* species are known to secrete immune-modulating substances. For example, immune cells are affected by spiralin, a well-characterized mycoplasmal lipoprotein that can stimulate the *in vitro* proliferation of human peripheral blood mononuclear cells and murine splenocytes. This stimulation of immune cells results in the secretion of pro-inflammatory cytokines (TNF-α, IL-1 or IL-6) (33).

Various respiratory illnesses, such as chronic asthma, airway inflammation, chronic pneumonia and other respiratory diseases, are known to be associated with mycoplasma infections. For example, *M. pneumonia* is a common cause of upper respiratory infections, and severe asthma is commonly associated with mycoplasma infections. Recent evidence has shown that certain mycoplasmas, such as *M. fermentans*, are unusually invasive and found within respiratory epithelial cells. Similar to certain *chlamydia* species, pulmonary macrophages appear unable to kill pathogenic *Mycoplasma* species (33).

In laboratory mouse, relatively few genetic studies of susceptibility to *M. pulmonis* infection have been performed (5, 11, 22, 23). Analysis of infected recombinant inbred strains specifically identified a region on chromosome (Chr) 4, in which the C57BL/6 (B6) mouse strain harbors a resistance allele, whereas C3H/He and BALB/c strains harbor a susceptibility allele (22). Moreover, infected congenic B6 mice that harbored a BALB/c-derived Chr 4 interval had increased mycoplasma loads in respiratory tract lavages and lung tissues compared to those of infected B6 mice. This observation confirmed the location of resistance locus on Chr 4, termed *M. pulmonis resistance 1 (Mpr1)*. However, these congenic B6 mice were still not as susceptible to infection as BALB/c mice, suggesting that there are B6 resistant alleles at other loci not identified by the recombinant inbred strain analysis (22).

M. pulmonis is a pathogenic agent responsible for numerous outbreaks of acute respiratory infection in rodents. However, the mechanism by which primary atypical pneumonia is caused by *M. pulmonis* is not clarified. Histopathologically, the bronchial and bronchiolar lumina are characteristically filled with polymorphonuclear leukocytes, and their walls have a mononuclear infiltrate with plasma cells (40). Therefore, it seems that other factors of the host may be involved. Experimental infections using mouse to examine the role of the cell-mediated immunity in the mycoplasmas were carried out mainly in B6, C3H and BALB/c mice (4, 5, 46). In DBA/2 (D2) mice which showed significantly higher mortality rate than C3H and BALB/C mice did (5), very limited information is available and the cell-mediated immunity to *M. pulmonis* has not been revealed. In this study, the cellular immune response was examined by using two inbred mouse strains, B6 (resistant) and D2 (susceptible), to exhibit the profiling of *M. pulmonis* infection, including bacteriological, histopathological, and immunological studies. Furthermore, quantitative trait locus (QTL) analysis was performed using these infected phenotypes as QTs to dissect genetic factors regulating the difference between these two inbred strains.

This study first examined and compiled the cellular immune responses to *M. pulmonis* infection in B6 and D2 mice. The results suggest that D2 mice are more susceptible than B6 mice to *M. pulmonis* infection due to a hyper-immune inflammatory response. Moreover, the study also elucidates infection mechanism of *M. pulmonis* and prevention of the infection that may have significant implications for the discovery of novel possible therapeutic targets and/or prognostic biomarkers complementing human studies, if new genes that contribute to the susceptibility/resistance are identified.

CHAPTER 1

Comparison of cellular immune responses between C57BL/6 and DBA/2 mice in response to *Mycoplasma pulmonis* infection

1. INTRODUCTION

Mycoplasma infection is a cause of respiratory disease in humans (52) and animals. Mycoplasmosis in humans accounts for 20 to 40% of all cases of pneumonia patients in the United States (53) and causes macrolide resistance problems (12, 37). In livestock, mycoplasma respiratory infections also cause a huge problem and make a significant economic loss in many countries (1, 2, 27). In addition, many kinds of animals can be infected with mycoplasmas and receive the severe impact from the infection.

M. pulmonis, a pleomorphic bacterium lacking a cell wall, is mainly implicated in murine respiratory mycoplasmosis (6, 7, 17) and can be transmitted by airborne droplet of nasopharyngeal secretion. Mycoplasma infection in laboratory mouse colonies causes severe problems to respiratory tract associated with rhinitis, otitis media, laryngotracheitis, and bronchopneumonia, leading to significant affects in the result of experiment (11). In terms of histopathology, mycoplasma infections are recognized by the accumulation of mononuclear and polynuclear cells along the respiratory airways (5, 10). Previous studies with different inbred mouse strains showed various susceptibility to this bacterial infection. For instance, infected B6 mice have bacterial load in their lungs 100-100,000 times lower than infected C3H mice (4) as well as lower gross lung lesions and lung histopathological lesions. However, the information mentioned above was mainly investigated in B6, C3H and BALB/c mice (10, 19, 22, 46). For D2 mice, very limited information is available and cellular immune responses to the bacteria are unknown. The results from my preliminary experiment among three inbred mouse strains, B6, C3H and D2 mice exhibited that B6 and D2 mice were the most different in symptoms caused by *M. pulmonis* infection. Therefore, it is worthwhile to determine the mechanisms of immune

responses that contribute to mycoplasmosis using B6 and D2 mice. This information may contribute to the development of new vaccines and comprehensive knowledge for mycoplasmosis in animals as well as humans. Both of innate and adaptive immune responses are associated with disease severity and susceptibility between the strains of mice (11). Inflammatory cellular and humoral responses have been used to investigate the host-pathogen interactions in various microbes (3, 24, 43, 48). Differences in the responses of immune cells and cytokines may be attributed to resistance or susceptibility in mice to mycoplasma infection.

Thus, in the current study, the cellular immune responses were examined by using two inbred mouse strains, B6 (resistant) and D2 (susceptible), to exhibit the profiling of the infection by observing disease-associated phenotypes such as lung histopathological lesions, propagation of bacteria in lung, lung cytological changes, cytokines levels in bronchoalveolar lavage fluid (BALF), and areas of lymphoid clusters (LCs) in mediastinal fat tissues (MFTs). Results indicated that D2 mice constantly had much greater number of colony-forming unit (CFU) of *M. pulmonis* in their lungs, greater severity of lung lesions, higher pulmonary infiltration of immune cells, and higher levels of cytokines in BALF. These results suggest that D2 mice are more susceptible than B6 mice to *M. pulmonis* infection due to a hyper-immune inflammatory response.

2. MATERIALS AND METHODS

2.1. Mice

Specific pathogen-free (SPF) 8-week-old female and male C57BL/6NCrSlc (B6) and DBA/2CrSlc (D2) mice were purchased from Japan SLC (Hamamatsu, Japan). All animals were kept under SPF conditions and infection experiments were conducted in the bio-safety level 3 facilities with sterile food and water *ad libitum*. Animal experimentation was conducted under the AAALAC International-accredited program and animal use protocol was approved by the President of Hokkaido University after review by the Institutional Animal Care and Use Committee (Protocol No. 16-0037).

2.2. Bacteria and infection

The CIEA-NH strain of *M. pulmonis* was kindly provided by Dr. Nobuhito Hayashimoto, Central Institute for Experimental Animals, Japan. Mycoplasma broth was made as follows; 21 g of mycoplasma broth base (BBL Microbiology Systems, Cockeysville, MD, USA), 5 g of D (+) - glucose (Wako Pure Chemical Industries, Ltd., Osaka, Japan), and 20 mg of phenol red (Wako) were dissolved with 750 ml of distilled water, autoclaved for 15 min, allowed to cool, and then 150 ml of heat-inactivated horse serum (GIBCO Laboratories, Grand Island, NY, USA), 100 ml of 25% fresh yeast extracts (Oriental Yeast Co., Ltd., Tokyo, Japan), 10 ml of 2.5% thallium acetate (Wako), and 1,000,000 units of ampicillin sodium salt (Sigma Chemical Company, Saint Louis, MO, USA) were added. After propagating *M. pulmonis* in the above broth, the stock cultures were divided into 1-ml aliquots and frozen at -80 °C until used. Mice from each strain (n = 5-6 per time point) were inoculated intranasally with 6.0×10^5 CFU of *M. pulmonis* in 30 μl of

inoculum after anesthetization with inhalation of isoflurane (Escain®;Pfizer Co., Ltd., Tokyo, Japan) followed by intraperitoneal injection of the mixture of 0.75 mg/kg body weight (b.w.) medetomidine (Domitor®Nippon Zenyaku Kogyo Co., Ltd., Koriyama, Japan), 4.0 mg/kg b.w. midazoram (Dormicum®, Astellas Pharma Inc., Tokyo, Japan), and 5.0 mg/kg b.w. butorphanol (Vetorphale®, Meiji Seika Pharma, Ltd., Tokyo, Japan) (20). The infected dose of inoculum used in the experiment was determined from preliminary experiment that showed the most difference of lesions between B6 and D2 mice after the infection. Control mice from each strain (n = 5 per time point) received the same volume of mycoplasma broth alone after the same anesthetization. Mice were daily observed for clinical signs, b.w., and body temperature. The samplings were performed at 7, 14, and 21 days post infection (d.p.i.) after euthanizing mice by inhalation of overdose of isoflurane (Escain®;Pfizer Co., Ltd.,).

2.3. Quantitative culture of *M. pulmonis* in lungs of infected mice

Mice were euthanized at the indicated time points. Lungs were removed aseptically and homogenized in 1 ml of mycoplasma broth with glass homogenizers (Sankyo Co., Ltd., Tokyo, Japan). Ten-fold serial dilutions were prepared and an aliquot of 10 μl of each dilution was plated onto PPLO agar medium, which was made by dissolving 35 g of PPLO agar (Becton Dickinson and Company, Sparks, MD, USA) with 750 ml of distilled water, autoclaved for 15 min, allowed to cool at 52-54 °C, and then 150 ml of heat-inactivated horse serum (GIBCO), 100 ml of 25% fresh yeast extracts (Oriental Yeast), and 1,000,000 units of ampicillin sodium salt (Sigma) were added. The total number of CFU per lung from each animal was determined under a stereomicroscope after incubation for 10 days at 37 °C in an incubator with 5% CO_2.

2.4. Determination of bacterial load by quantitative PCR

The bacterial replication level in the lung was determined by quantitative real-time PCR. Briefly, mice from each group were sacrificed at 7, 14, and 21 d.p.i. and whole lungs were collected by aseptic technique. The individual lung from each mouse was homogenized in 1 ml of mycoplasma broth with glass homogenizers (Sankyo Co., Ltd.). The homogenized lung suspension (300 μl) was used for DNA extraction. DNA was extracted by adding 500 μl of lysis buffer [10 mM Tris (Wako), 10 mM ethylenediaminetetraacetic acid (EDTA)-2Na (Wako), 150 mM NaCl (Wako), and 0.1% sodium dodecyl sulfate (Wako)] and 5 μl of 10 mg/ml proteinase K (Invitrogen, Carlsbad, CA, USA) and incubating for 3-4 h at 54 °C for lysis. To detect *M. pulmonis* DNA, total DNA was used as a template with PCR primers, which were designed based on the conserved spacer region encompassing the 16S and 23S rRNA gene of *M. pulmonis* (18, 26, 49). The primers used were FN2 (5′-ACCTCCTTTCTACGGAGTACAA-3′) and R2 (5′-GCATCCACTACAAACTCTT-3′) (47). Quantitative real-time PCR was performed using the FastStart Essential DNA Green Master (Roche Diagnostics Corporation, Indianapolis, IN, USA) and LightCycler96 instrument (Roche). A reaction mixture (10 μl) contained 1 μM of each primer, 5 μl of FastStart Essential DNA Green Master (Roche), and 50 ng of genomic DNA template. Amplification conditions consisted of 45 cycles of denaturation at 95 °C for 10 s, annealing at 60 °C for 10 s, and extension at 72 °C for 30 s. The products were analyzed with the accompanying software and the amount of bacterial DNA in each sample was calculated using a standard curve, which was plotted serial ten-fold dilutions of template with known concentration.

2.5. Histopathological analysis

Whole lungs and MFT from individual mouse were removed, and then fixed in 4% paraformaldehyde to inflate and preserve lung architecture. After overnight fixation, specimens were washed in distilled water followed by dehydrated in graded alcohol and embedded in paraffin. The paraffin-embedded specimens were sectioned at a thickness of 3 μm, and subsequently deparaffinized, rehydrated, and stained with hematoxylin and eosin (H&E) to observe under a light microscope and examined lesion severity. For lung, ten sections were cut and five fields were randomly observed in each slide. The degree of distribution and severity of inflammatory infiltration/structural alterations were determined on the basis of the characteristic lesions of mycoplasmosis examined around small airways and adjacent blood vessels. Scores (scale of 1 to 6) refer to normal, 1; slight/mild, 2; moderate, 3; severe, 4; and highly severe, 6. Pathological scores for the lung sections were averaged and determined as the pathological index.

Immunohistochemical analysis for Gr1 (Ly-6G) and Iba1 was performed in lung tissue of both B6 and D2 mice to detect neutrophils and macrophages, respectively. Immunohistochemical procedures were performed according to the method described previously (14). Briefly, following deparaffinization, heat-induced antigen retrieval was applied using 0.1% pepsin in 0.2 ml HCl at 37 °C for 5 min and 10 mM citrate buffer (pH 6.0) at 105 °C for 20 min. Then, following endogenous peroxidase blocking with 0.3% hydrogen peroxide in absolute methanol at room temperature for 20 min, the sections were incubated with 10% normal goat serum for 1 h at room temperature. Then, the sections were incubated overnight with the specific primary antibody, rat anti-Gr1 (Rand D system, Minneapolis, USA) or rabbit anti-Iba1 (Wako, Osaka, Japan), diluted in phosphate-buffered saline (PBS) (pH 7.2) containing 1.5% bovine serum albumin, at dilution of 1:800 or 1:1,200, respectively. Then the sections were incubated with

biotin-conjugated secondary antibody, goat-anti-rat IgG for rat anti-Gr1 or goat-anti-rabbit IgG for rabbit anti-Iba1, for 1 h at room temperature, then with streptavidin-peroxidase for 30 min. Between the various steps, sections were thoroughly rinsed in PBS 3 times for 5 min each. The immunopositive reactions were visualized with 3,3′-diaminobenzidine-H_2O_2 solution for 2 min. Then, the sections were washed in distilled water, lightly stained with Mayer's hematoxylin for 30 s, dehydrated, and mounted. All sections were photographically captured using a fluorescence microscope, BZ-X710 (Keyence, Osaka, Japan).

For MFT, the light micrographs of H&E-stained MFT sections from each mouse were scanned using a NanoZoomer-XR Digital slide scanner (Hamamatsu Photonics K.K., Hamamatsu, Japan). The area of LC and the total areas of the mediastinal white adipose tissue within the MFT were measured using a NDP.view2 Viewing software (ver. 2.6.13, Hamamatsu Photonics) and the ratio of LC area to total MFT area was calculated.

2.6. Brochoalveolar lavagefluid (BALF) collection and cytology

Mice were euthanized by inhalation of overdose of isoflurane at the indicated time point and BALF was collected as described previously (9). Briefly, a sterile 20-gauge animal feeding needle (Fuchigami Instruments Co., Ltd., Kyoto, Japan) was inserted through the mouth and larynx into the lumen of the trachea. The lungs were then slowly lavaged *in situ* with three separated 300 μl of sterile PBS, pH 7.2. The BALF was centrifuged at 300 x g at 4 °C for 5 min, and then the supernatants were collected and stored at -80 °C for the cytokine analysis. The cell pellet was suspended in 1.5 ml of distilled water, placed for 10 s, and then added 500 μl of 0.6 M KCl and mixed by inverting. Suspensions were centrifuged at 300 x g at 4 °C for 5 min and the supernatants were discarded. The cell pellets were resuspended by adding 500 μl of sterile saline

(0.9% NaCl) with 2.6 mM EDTA and mixed by inverting, and then total count of viable leukocytes was determined by using a heamocytometer (Erma Inc., Tokyo, Japan). To determine differential cell count, 200 μl of the BALF cell suspensions were loaded onto a Shandon™ EZ Single Cytofunnel (Thermo Fisher Scientific, Cheshire, UK) and centrifuged for 10 min at 108 x g. Finally, the slides were dried at room temperature and stained with a Diff-Quick Staining Kit according to the manufacture's protocol.

2.7. Cytokine analysis

A Bio-Plex Pro Mouse Cytokine Th17 Panel A 6-Plex (Bio-Rad, Hercules, CA, USA) was used to evaluate the cytokine levels in BALF supernatant. IFN-γ, IL-1β, IL-6, IL-10, IL-17A and TNF-α were measured according to the manufacture's protocol. Concentration of each cytokine was determined and calculated using a beads assay on the Bio-Rad Bio-Plex 200 System (Bio-Rad) and Bio-Plex Manager version 6.0 software, respectively.

2.8. Statistical analysis

The results of the various groups were compared by using an analysis of variance (ANOVA). Scheffe's post-hoc test was used for multiple comparisons when a significant difference was observed by ANOVA ($P < 0.05$). All values were represented as mean ± standard error (SE). Values of $P \leq 0.05$ were considered statistical significance.

3. RESULTS

3.1. Disease severity and development of lung pathology in infected B6 and D2 mice

To characterize the development of mycoplasmosis in B6 and D2 mice, age- and sex-matched mice of each strain were infected with *M. pulmonis*, and then body weight loss and histological change were evaluated (n = 5-6 per time point) at 7, 14, and 21 d.p.i.. As a control group, mice were inoculated with mycoplasma broth only. *M. pulmonis*-infected D2 mice showed significant decline in weight ($P < 0.05$) at 7 d.p.i. compared to infected B6 mice as well as broth-inoculated control mice (Fig. 1). Namely, D2 mice exhibited severe b.w. loss, nearly 30% from the initial b.w..

In the pathological examination, lungs were collected from infected B6, D2, and broth-inoculated control mice at 7, 14, and 21 d.p.i.. Pathological changes were examined through H&E staining of lung sections. D2 mice but not B6 mice distinctly showed gross lung lesions following *M. pulmonis* infection. The gross lesions in infected D2 mice showed moderate to severe pulmonary hemorrhage and consolidation (Fig. 2). The histopathological lesion was suppurative bronchopneumonia with squamoid changes of the respiratory epithelium. Prominent cuffing of bronchi, bronchioles and blood vessels by lymphoid cells as well as parenchymal lesions consisting of alveoli filled with neutrophils and macrophages were common in most of infected D2 mice at all time points (Fig. 3A, B, and C). On the other hand, infected B6 mice showed limited lesions with a few lymphoid cells around the vessels and airways. Infected D2 mice had extensive lymphoid infiltrates such as macrophages and neutrophils around bronchi, and mixed inflammatory response in alveoli (Fig. 3B and C). These differences included

increased exudate, epithelial hyperplasia, and lymphoid hyperplasia in the lungs. There was no difference observed between males and females in both strains (Figs. 9 and 10).

The inflammatory dynamics of the pulmonary epithelium were investigated by comparing lung histopathological changes after bacterial infection. The representative histopathology sections taken from each group of mice demonstrated the relative degree of pathological changes that developed in the lungs after the infection. The lung pathological index scores were significantly higher ($P < 0.01$) in infected D2 mice than in infected B6 mice at all time points (Fig. 3D) and there was no sexual difference (Fig. 10).

The stereomicroscopic observation of the MFTs were examined. The result from all mice showed dark-stained regions that varied in shape and size and these regions were confirmed as LCs by subsequent histological examination (Fig. 4A). Especially, the MFTs of infected B6 mice had a smaller number of LCs compared with infected D2 and broth-inoculated control mice at 14 and 21 d.p.i.. These observations were confirmed by image viewing. The ratios of LC area to total MFT area in infected B6 mice were not significantly higher than infected D2 mice at 7 d.p.i. but significantly lower ($P < 0.005$) than infected D2mice at 14 and 21 d.p.i (Fig. 4B).

3.2. Cytology in BALF of infected B6 and D2 mice

Cytology was performed using the suspension of BALF samples from each time point. The number of infiltrated cells was higher in infected D2 than in infected B6 and broth-inoculated control mice at all time points (Fig. 5). After counting the number of each cell type, it was revealed that the total cell counts in infected D2 mice were significantly higher ($P < 0.005$) than in infected B6 and broth-inoculated control mice at all time points (Fig. 6A). For the differential cell count, infected D2 mice had a higher population of neutrophils (Fig. 6B) and

macrophages (Fig. 6C) compared with infected B6 ($P < 0.05$) and broth-inoculated control mice ($P < 0.01$). However, lymphocyte population was not significantly different among infected B6, infected D2, and broth-inoculated control mice (Fig. 6D).

3.3. Quantification of bacteria in lungs of infected B6 and D2 mice

To determine whether the burden of infection corresponded with disease severity, the numbers of bacteria were determined in the lungs of mice. There were significant differences in the number of bacteria recovered from the lung between infected B6 and D2 mice (Fig. 7A). At 7 and 14 d.p.i., infected D2 mice had higher ($P < 0.01$) CFU per lung 10^2- to 10^4-fold more than infected B6 mice. However, at 21 d.p.i., the CFU per lung was not statistically different between infected B6 and D2 mice. Next, the quantity of *M. pulmonis* DNA in lung was determined by quantitative real-time PCR. Infected D2 mice also showed higher ($P < 0.01$) amount of bacterial DNA in lung than infected B6 mice (Fig. 7B). These results affirmed that the D2 mouse was the susceptible strain to *M. pulmonis* infection. The number of bacteria recovered from lung tissues was not different with the sex at the indicated time points (Fig. 11).

3.4. Cytokine level in BALF of infected B6 and D2 mice

To exhibit the inflammatory response in lung to the mycoplasma infection, cytokine levels in the supernatant of BALF was measured. The infection induced the expression of pro- and anti-inflammatory cytokines in the lung (Fig. 8). At 7 d.p.i., IL-1β, IL-6, and TNF-α levels in infected D2 mice were significantly higher ($P < 0.05$) than in infected B6 mice. IL-17A level in infected D2 mice was higher with high significance ($P < 0.005$) compared with infected B6 mice. Remarkably, at 14 d.p.i. IL-6, IL-17A, and TNF-α levels were significantly higher ($P < 0.01$) in

infected D2 mice compared with infected B6 mice. In contrast, the level of IL-1β in infected B6 mice was significantly higher ($P < 0.05$) than in infected D2 mice. Interestingly, at 21 d.p.i. TNF-α and IL-17A levels in infected D2 mice were significantly higher ($P < 0.05$ and $P < 0.01$, respectively) than infected B6 mice. Moreover, the IL-17A level exhibited the highest level at 7 d.p.i. and declined at 14 and 21 d.p.i.. The results confirmed that specific cytokine levels correlate with the bacterial load in lung of infected mice. Nevertheless, in this analysis had no any significant elevation of IL-10 and IFN-γ in infected B6 and D2 mice and found that the level of both cytokines was similar to the normal baseline level of broth-inoculated control mice (Fig. 8).

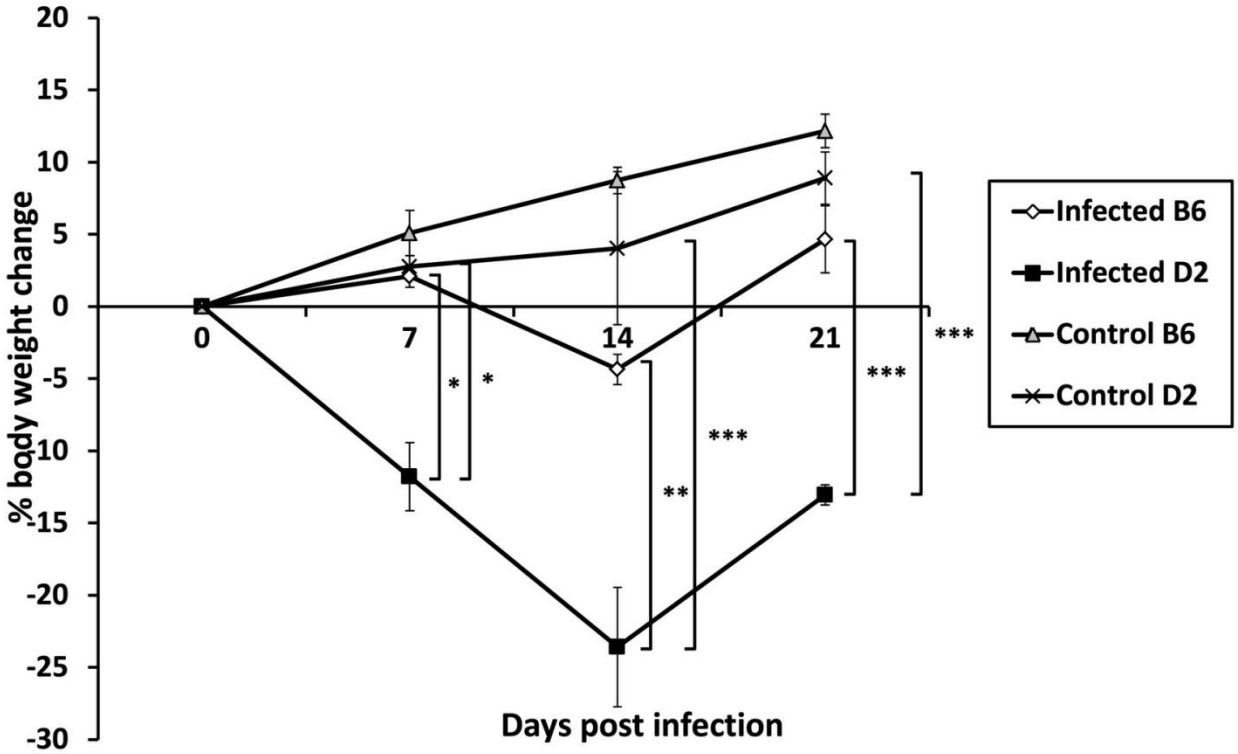

Fig. 1. Body weight changes in infected female B6, infected female D2, and control female mice after *M. pulmonis* infection. The time course of changes was shown in percentage of b.w. loss in mice (n = 5-6 per group) infected with 6×10^5 CFU of *M. pulmonis*. *, **, and *** indicate $P < 0.05$, $P < 0.01$, and $P < 0.005$, respectively.

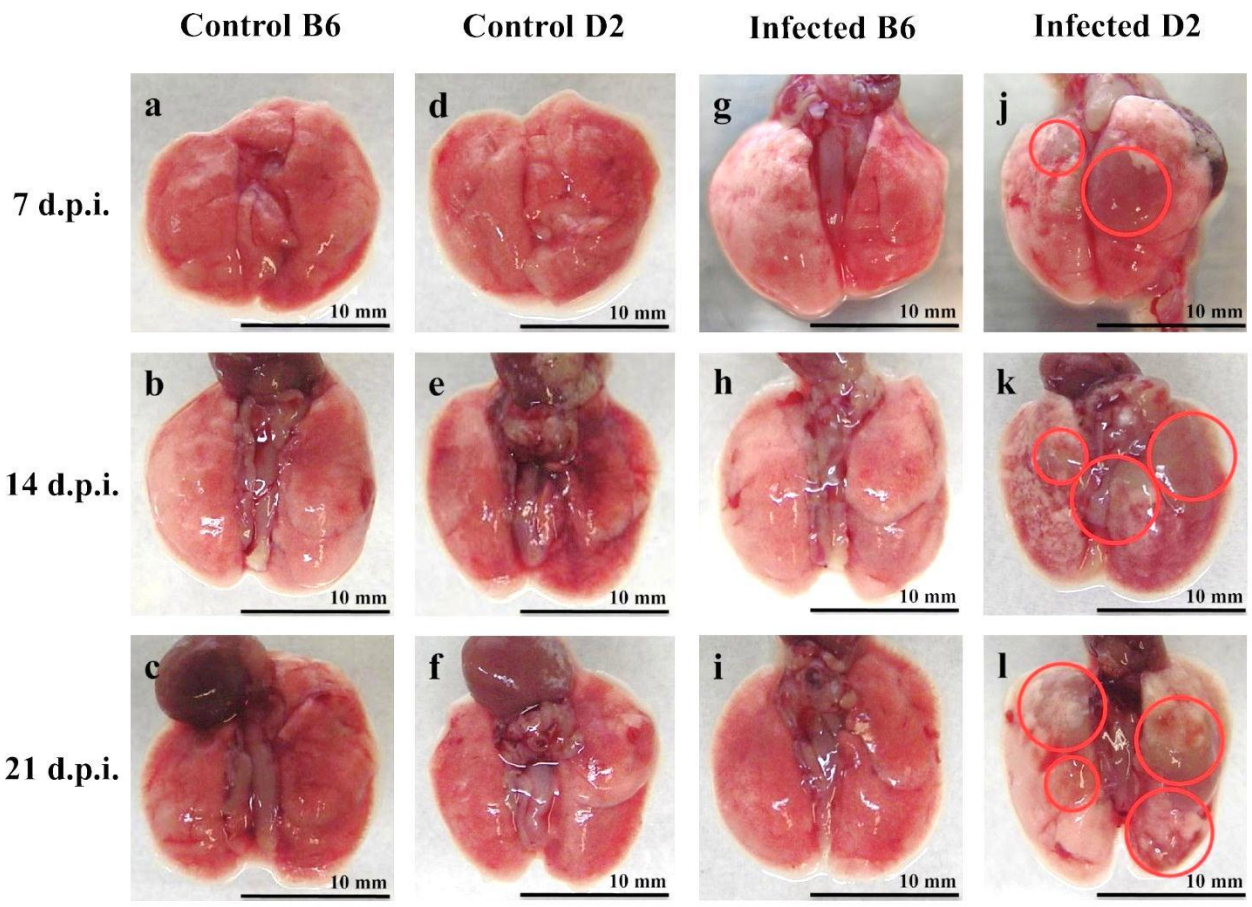

Fig. 2. Gross lung lesions in infected female and control female mice after *M. pulmonis* infection. Mice were infected with 6×10^5 CFU of *M. pulmonis*. Results are shown as representatives at each time point ($n = 5$-6 per group) of lungs from control B6 (a-c), control D2 (d-f), infected B6 (g-i), and infected D2 (j-l) mice. Infected D2 mice showed severe pulmonary hemorrhage and consolidation (red circles in j-l) at all time points. In contrast, no gross lung lesions were observed in control B6, control D2, and infected B6 mice. All scale bars indicate 10 mm.

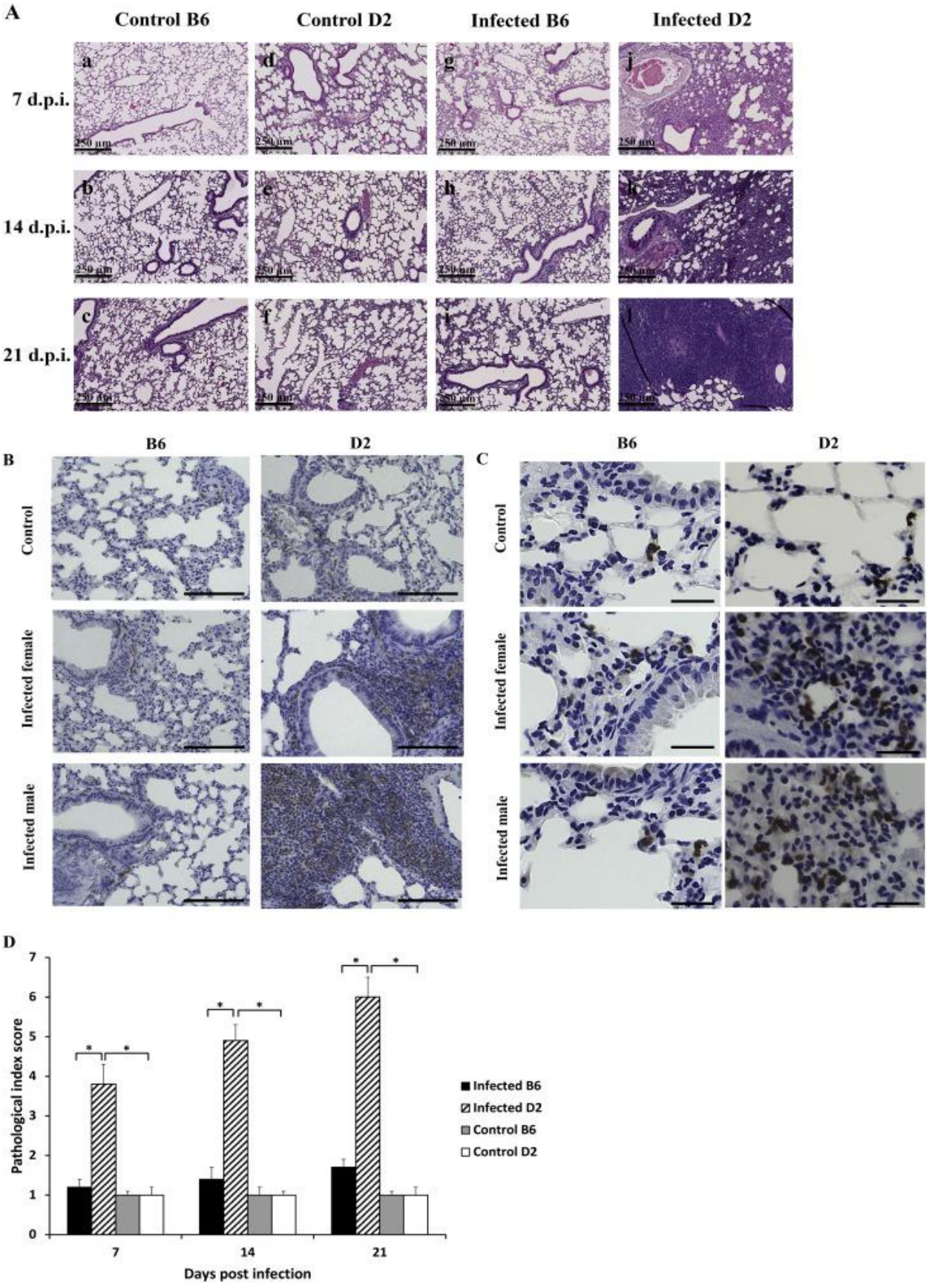
A
Control B6
Control D2
Infected B6
Infected D2
7 d.p.i.
14 d.p.i.
21 d.p.i.
a
b
c
d
e
f
g
h
i
j
k
l
250 μm
B
B6
D2
Control
Infected female
Infected male
C
B6
D2
Control
Infected female
Infected male
D
Pathological index score
0
1
2
3
4
5
6
7
7
14
21
Days post infection
Infected B6
Infected D2
Control B6
Control D2
*

Fig. 3. (A) Histopathological observation of lung sections in infected female and control female mice after *M. pulmonis* infection. Results are shown as representatives of light microscopic images of H&E-stained lung sections collected from control B6 (a-c), control D2 (d-f), infected B6 (g-i), and infected D2 (j-l) mice ($n = 5$-6 per group) at the indicated time points after infection with 6×10^5 CFU of *M. pulmonis*. Infected D2 mice (j-l) showed extensive lymphoid infiltration around bronchi, neutrophils in lumen of airways, and mixed inflammatory response in alveoli. Infected B6 mice (g-i) showed lesions limited to a few lymphoid cells around the vessels and airways. The lungs of control mice (a-f) showed mild lymphoid cell infiltration around the vessel and airways. All scale bars indicate 250 μm. (B) Immunohistochemical staining of Iba1 (macrophage marker) in the lung after two weeks of *M. pulmonis* infection. Infected D2 mice showed numerous Iba-positive cells (stained brown). All scale bars indicate 100 μm. (C) Immunohistochemical staining of Gr1 (neutrophil marker) in the lung after two weeks of *M. pulmonis* infection. Infected D2 mice showed numerous Gr1-positive cells (stained brown). All scale bars indicate 30 μm. (D) Lung pathological index score in infected female B6, infected female D2, and control female mice after *M. pulmonis* infection. The histogram showed the pathological index score of lung lesions by H&E staining in each group at the indicated time points. Results are expressed as the mean ± SE. * indicates $P < 0.01$.

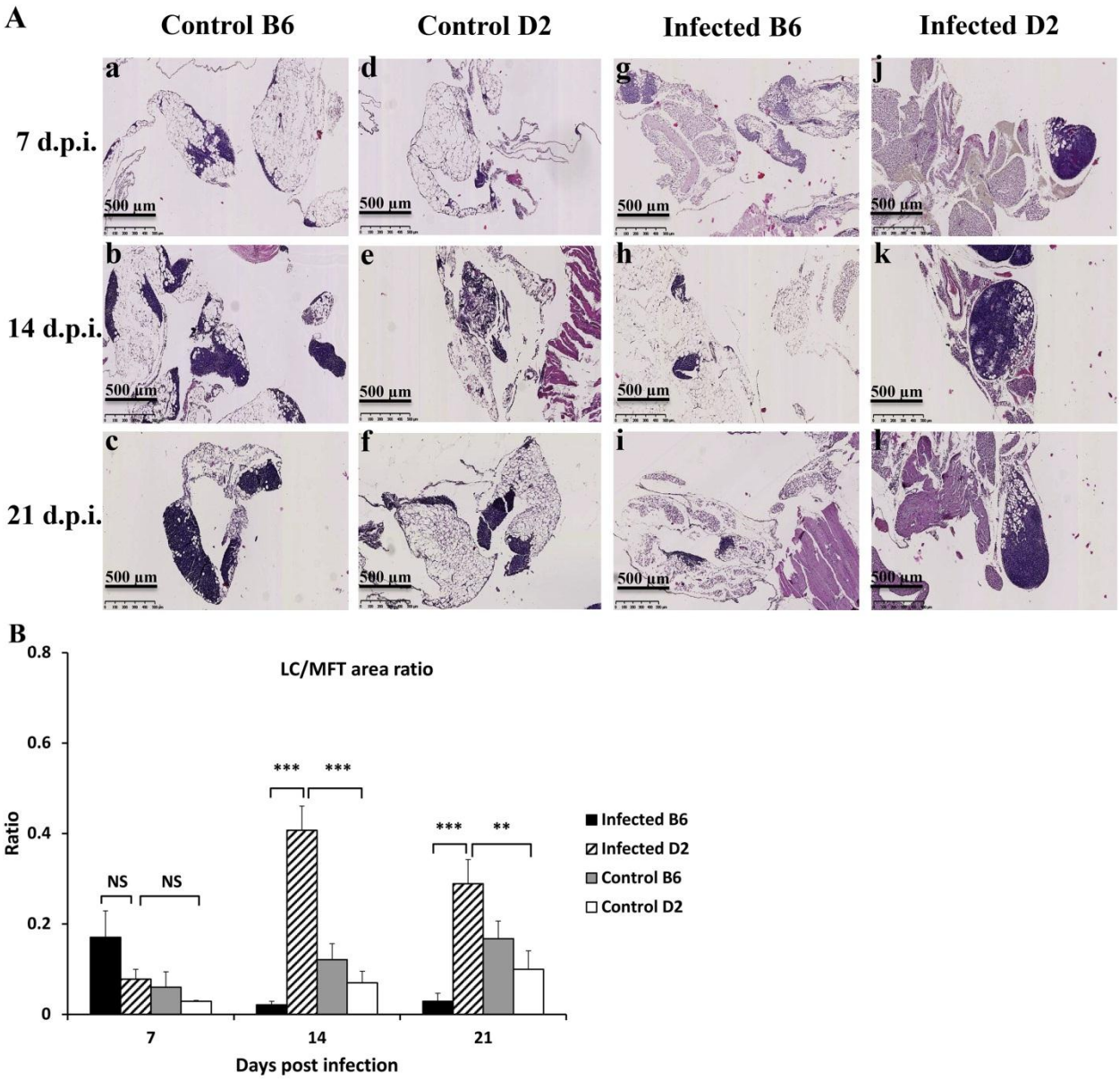

Fig. 4. (A) Histological features of LCs in MFT in infected female and control female mice after *M. pulmonis* infection. Representative light micrographs of H&E-stained MFT sections of control B6 (a-c), control D2 (d-f), infected B6 (g-i), and infected D2 (j-l) mice ($n = 5$-6 per group) collected at the indicated time points after infection with 6×10^5 CFU of *M. pulmonis*. The accumulation of mononuclear cells is visible in the MFT. Larger areas of LCs are visible in infected D2 mice (j-l) compared with infected B6 (g-i) and control mice. All scale bars

indicate 500 μm. (B) Percentage of LC area in the total MFT area in the H&E-stained sections in infected female B6, infected female D2, and control female mice after infection with 6×10^5 CFU of *M. pulmonis*. Results are expressed as the mean values of the ratio in the experimental groups. **, and *** indicate $P < 0.01$ and $P < 0.005$, respectively. NS; not significantly different.

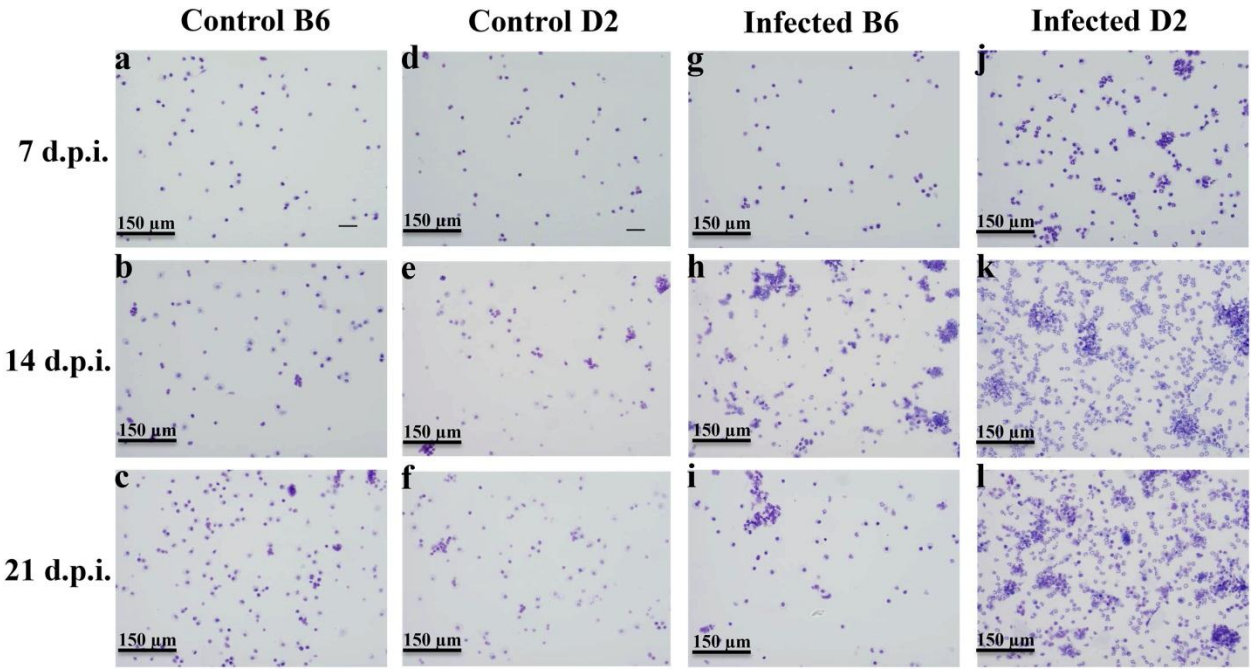

Fig. 5. Cell cytology slides from BALF in infected female and control female mice after *M. pulmonis* infection. Results are shown as representative photomicrographs of Diff-Quick- stained cytospin slides of control B6 (a-c), control D2 (d-f), infected B6 (g-i), and infected D2 (j-l) mice ($n = 5$-6 per group) at the indicated time points after infection with 6×10^5 CFU of *M. pulmonis*. The accumulation of mononuclear cells is visible in the slide. More inflammatory cells infiltrated are visible in infected D2 mice (j-l) compared with infected B6 (g-i) and control mice. All scale bars indicate 150 μm.

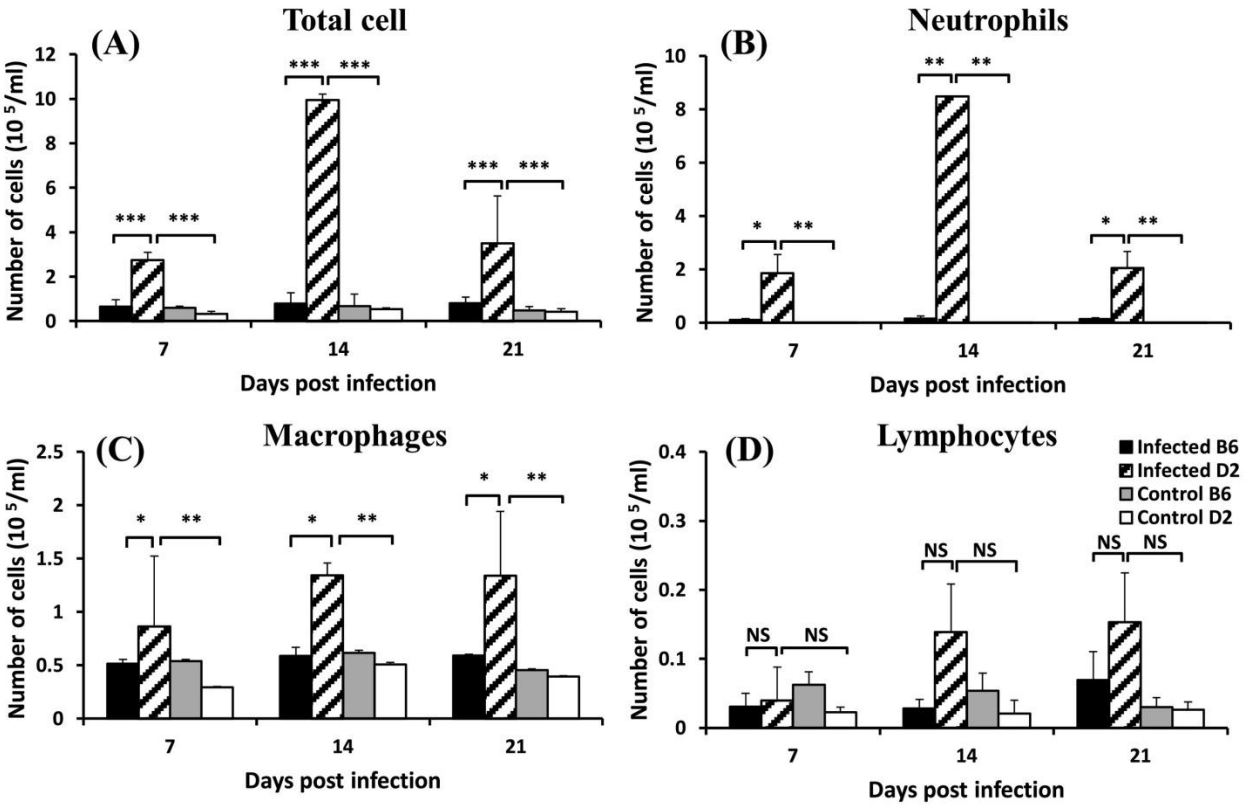

Fig. 6. Total and differential white blood cell counts in BALF in infected female B6, infected female D2, and control female mice after *M. pulmonis* infection. (A), total cells; (B), neutrophils; (C), macrophages; and (D), lymphocytes. Results are expressed as the mean cell counts of the data ($n = 5$-6 per group). *, **, and *** indicate $P < 0.05$, $P < 0.01$, and $P < 0.005$, respectively. NS; not significantly different.

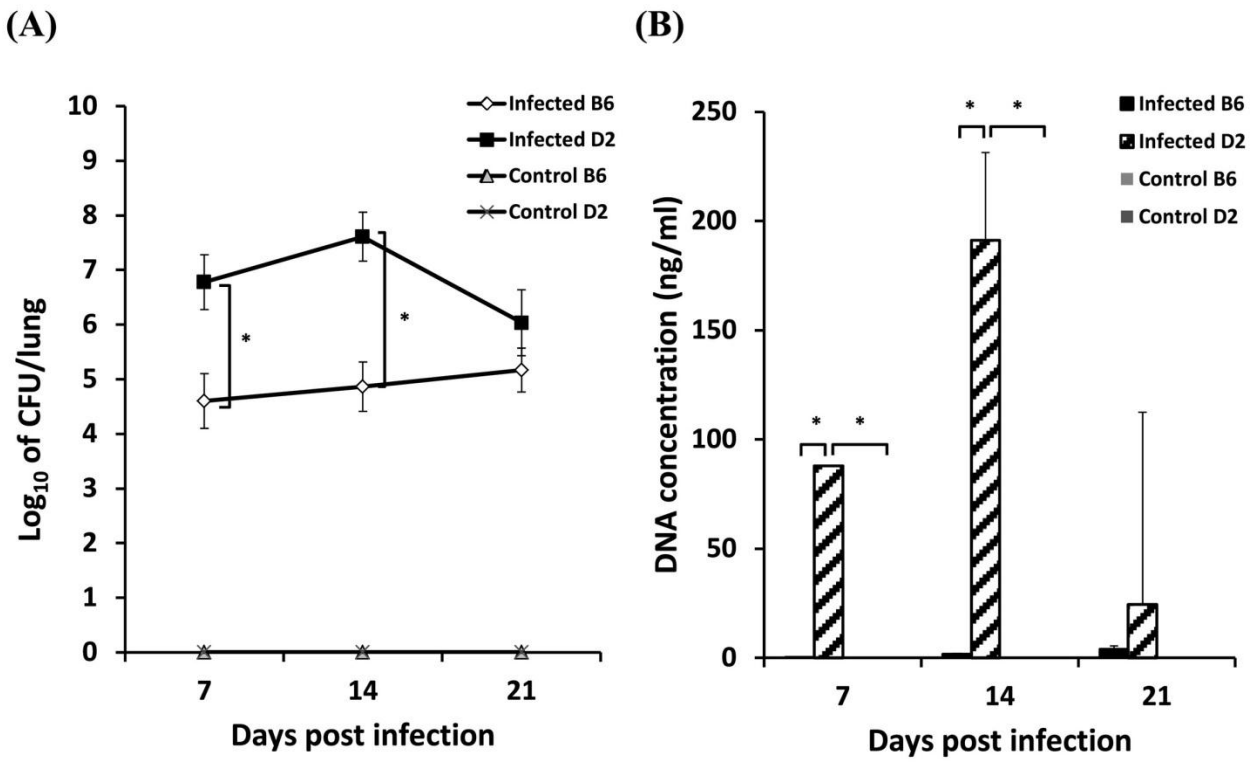

Fig. 7. Amounts of *M. pulmonis* in lungs of infected female B6, infected female D2, and control female mice after *M. pulmonis* infection. (A) CFU of *M. pulmonis* in the culture of whole lung homogenates. (B) *M. pulmonis* DNA concentrations in the homogenized lungs determined by real-time PCR. * indicates $P < 0.01$.

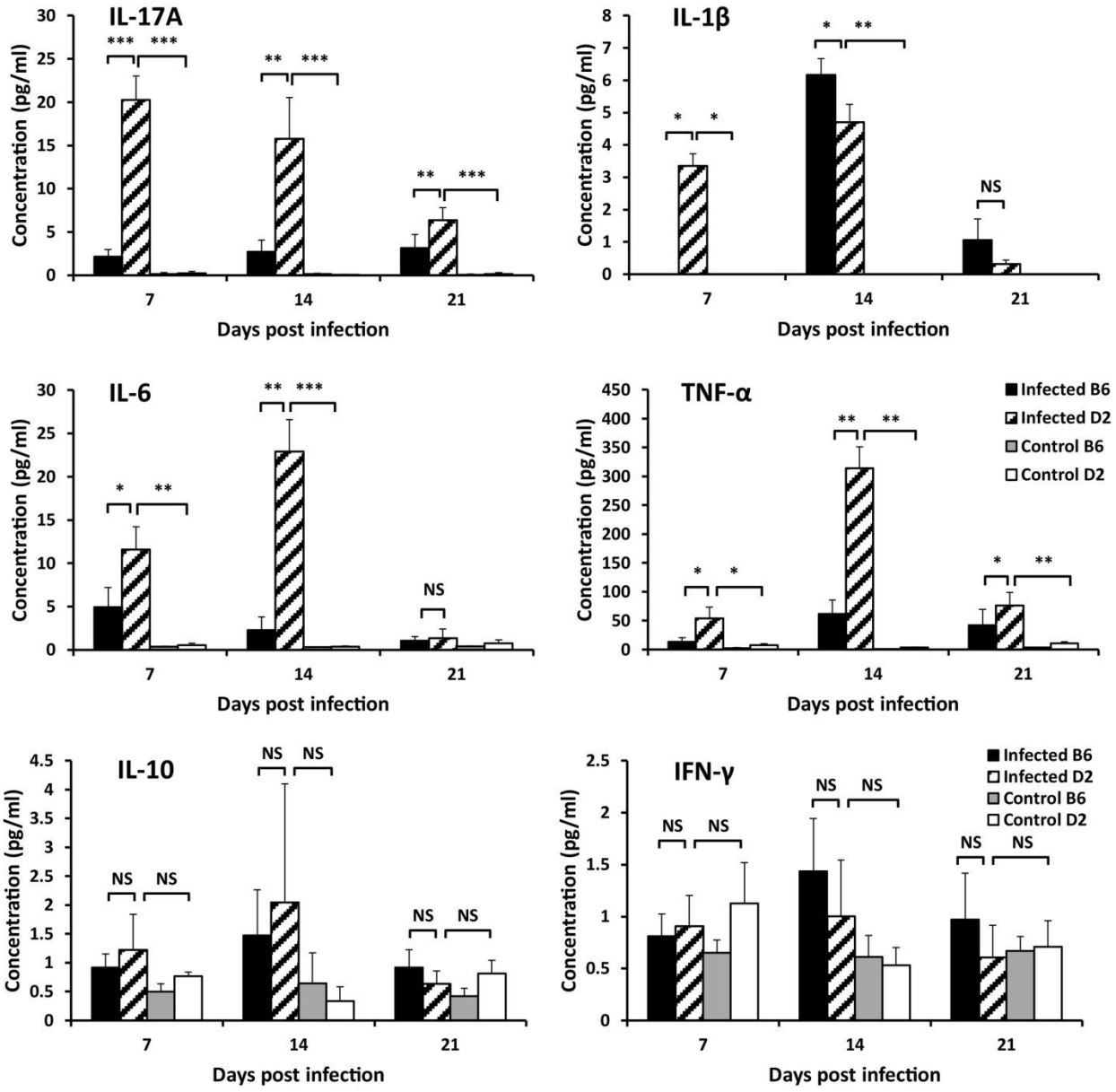

Fig. 8. Pulmonary cytokine levels in infected female B6, infected female D2, and control female mice after *M. pulmonis* infection. Cytokine concentrations in BALF were determined by the Luminex bead assay. Results are expressed as the mean values of samples ($n = 5$-6 per group). Marks of the columns are in common with each small figure. *, **, and *** indicate $P < 0.05$, $P < 0.01$, and $P < 0.005$, respectively. NS; not significantly different.

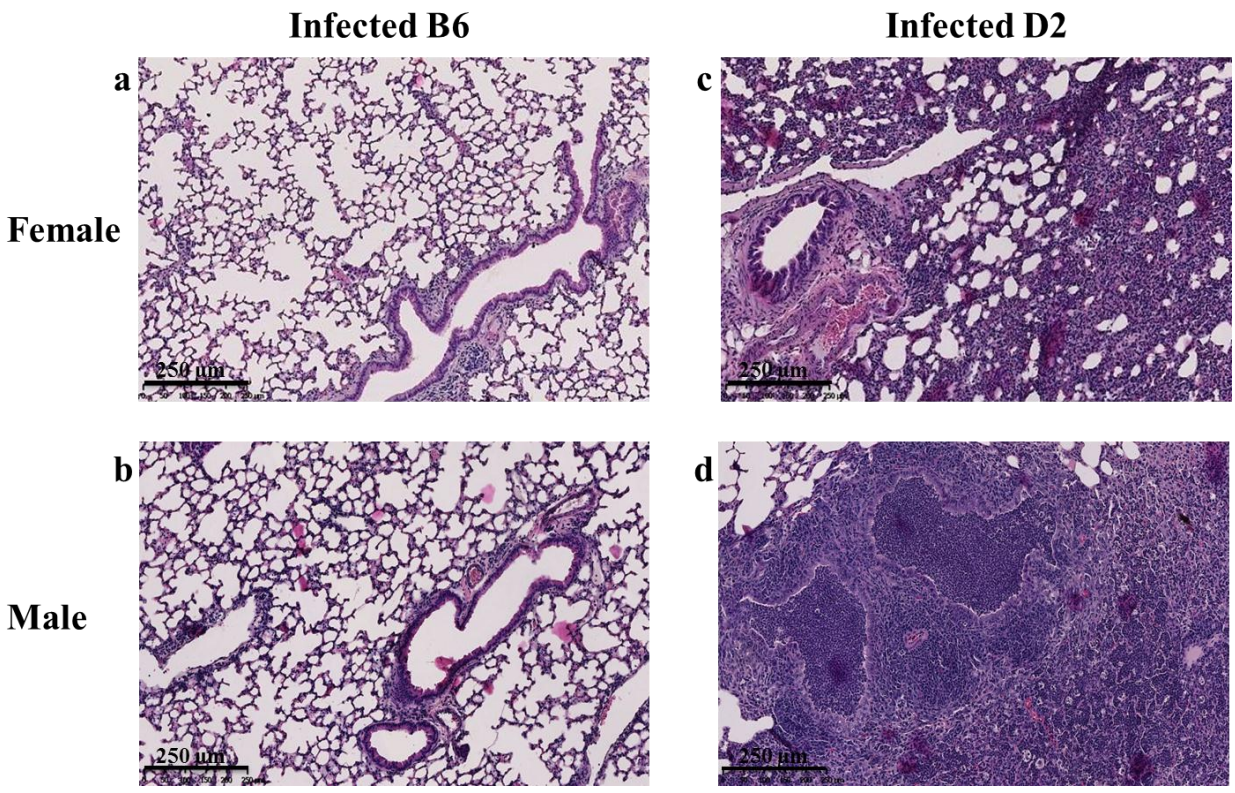

Fig. 9. Representative of histopathological observation of lung sections in infected B6 female, infected B6 male, infected D2 female, and infected D2 male mice after *M. pulmonis* infection. Representative light microscopic images of H&E-stained lung sections collected from 14 days after *M. pulmonis* infection. Infected B6 female (a), infected B6 male (b), infected D2 female (c), and infected D2 male (d) mice (n = 5-6 per group). Infected D2 female and male mice (c and d) showed extensive lymphoid infiltration around bronchi, neutrophils in lumen of airways, and mixed inflammatory response in alveoli. Infected B6 female and male mice (a and b) showed lesions limited to a few lymphoid cells around the vessels and airways. All scale bars indicate 250 µm.

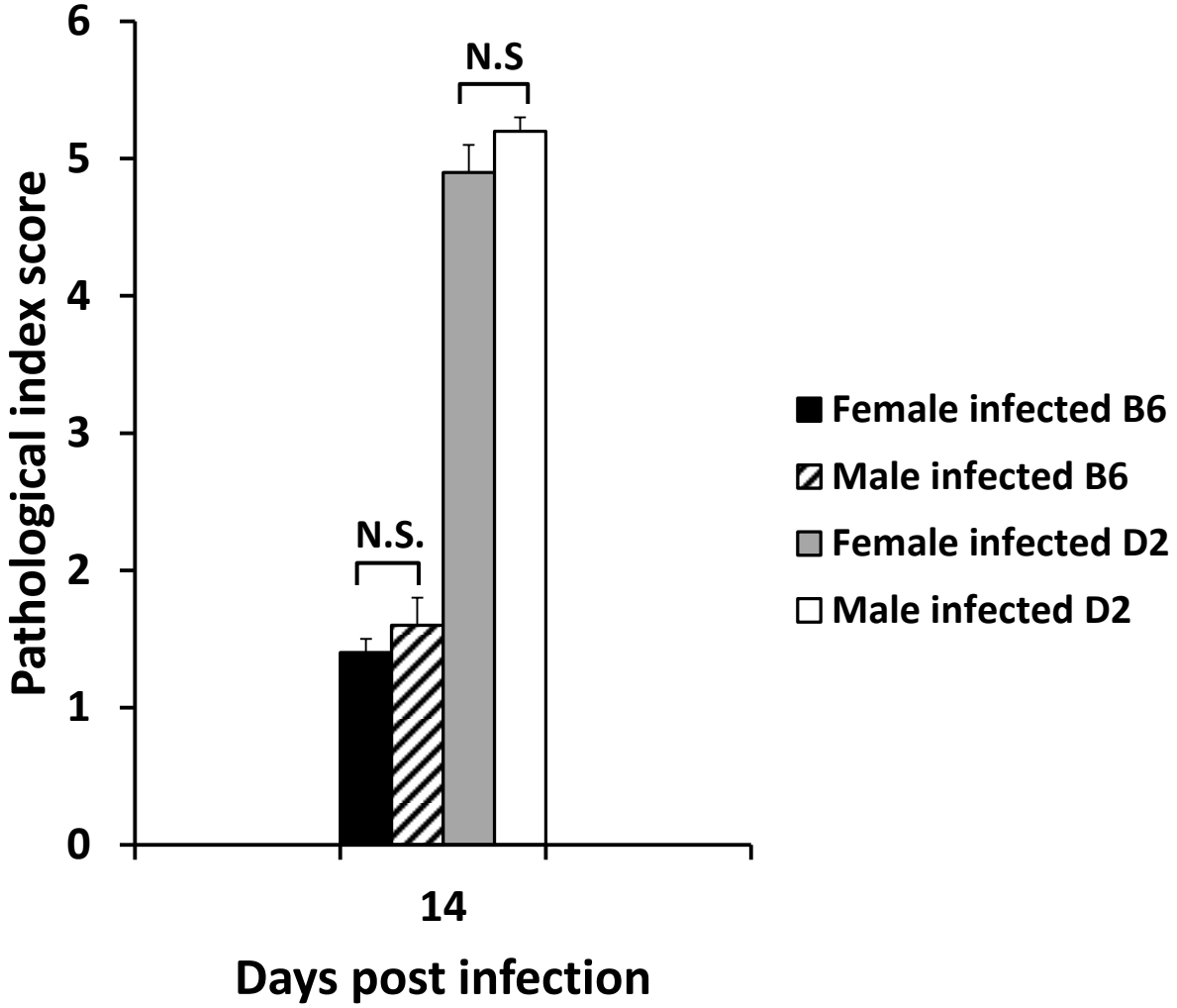

Fig. 10. Lung pathological index score in infected B6 female, infected B6 male, infected D2 female, and infected D2 male mice after *M. pulmonis* infection. The histogram showed the pathological index score of lung lesions by H&E staining in each group at 14 days after the infection. Results are expressed as the mean ± SE. NS; not significantly different.

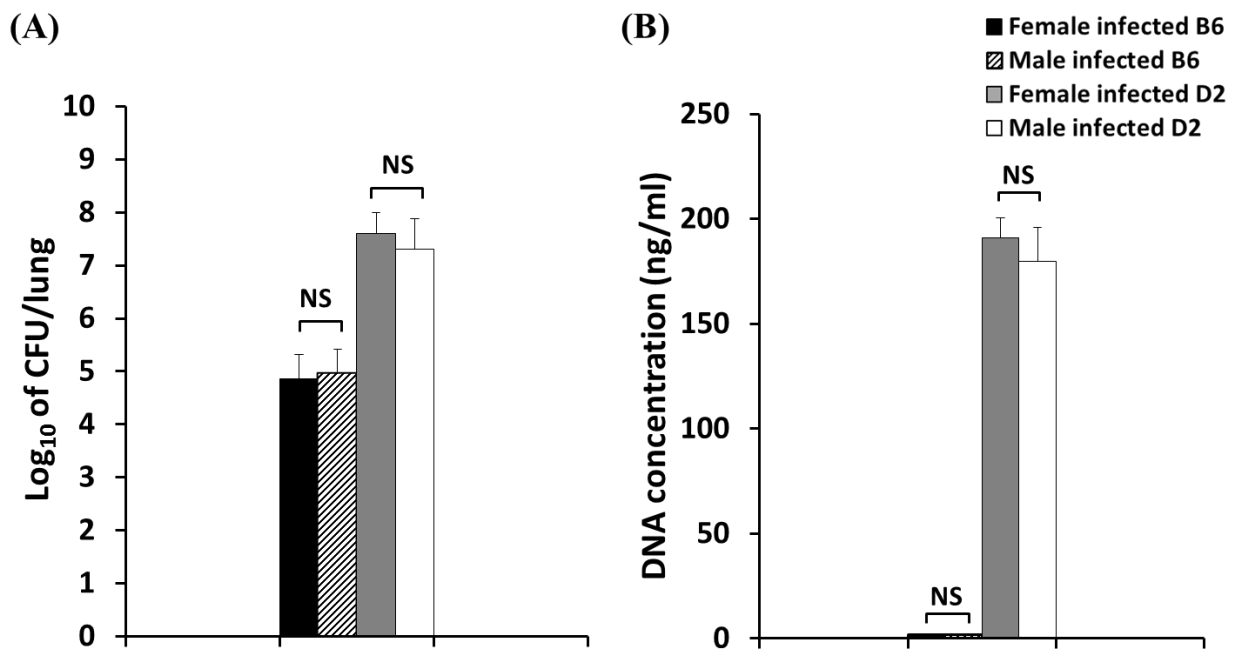

Fig. 11. Amounts of *M. pulmonis* in lungs of infected B6 female, infected B6 male, infected D2 female, and infected D2 male mice at 14 days after *M. pulmonis* infection. (A), CFU of *M. pulmonis* in the culture of whole lung homogenates. (B), *M. pulmonis* DNA concentrations in the homogenized lungs determined by real-time PCR. NS; not significantly different.

4. DISCUSSION

The host-pathogen interplay is related to many factors. The genetic background of the animal is one of the important factors that control an immune response. In several infectious diseases, it has been demonstrated that the different strains of animals show different susceptibility caused by different immune responses (3, 38, 43, 55). In laboratory rodents, distinct difference in the response to the bacterial as well as viral infection was found. The B6 mouse was known to be resistant to the Sendai virus infection (42) as well as mycoplasma infection (11). On the other hand, the D2 mouse is susceptible to the Sendai virus and mycoplasma infection. Various experiments of *M. pulmonis* infection using susceptible and resistant strains of mouse were performed (46). However, the mechanism of the susceptibility and resistance is still unclear. Furthermore, little is known about the profiling of immune responses. In this study, the infection experiment was conducted to display the immune responses to the infection including b.w. loss, histopathology of lung, bacterial load in lung tissues, cell cytology, and cytokine levels in BALF as well as histology of MFTs.

In the present study, the disease severity was evaluated in both susceptible D2 and resistant B6 mice after *M. pulmonis* infection. There was a clear association between disease pathogenesis and the quantity of bacteria recovered from lungs. The susceptible D2 mice distinctly expressed gross lung lesions and histological lung lesions as determined by macroscopic and microscopic examinations after the infection. In contrast, there was a very limited histological lesion in resistant B6 mice. Results showed that the period of pulmonary immune response to *M. pulmonis* infection in D2 mice was early and intense (Fig. 2 and Fig. 3) consistent to the result of cytokine levels and bacterial load in lung as reported previously (5, 46).

The results from the CFU counting were highly correlated with data obtained by quantitative real-time PCR. The number of *M. pulmonis* recovered from lungs in D2 mice was 1,000 times higher than that from B6 mice (Fig. 7). Bacterial burden may cause pro-inflammatory cytokine induction and result in the strain difference in the severity of the infection. *M. pulmonis* infection strongly induced cytokines such as IL-1β, IL-6, TNF-α with their peak observed at 14 d.p.i., and IL-17A level with its peak at 7 d.p.i., while other cytokines did not differ significantly between infected and control mice (Fig. 8). It has been reported that IL-1β, IL-6, and TNF-α augment IL-17A production (8, 30). Results are consistent with these previous reports. The elevation of these cytokines may contribute to the exacerbated disease observed in D2 mice. The high expression of these cytokines was consistent with the recruitment of inflammatory cells, including neutrophils, macrophages, and lymphocytes to the lung of infected mice. The over induction of these cytokines in D2 mice might cause the over response to the infection and resulted in excessive inflammatory reaction that can be observed in the histopathological sections of lung tissues (Fig. 3). Interestingly, B6 mice showed significant increase in IL-1β level higher than D2 mice at 14 d.p.i. (Fig. 8), and it may be inefficient to control of inflammation by reducing cytokine production (50, 51) and blocking of the bacterial growth in lung (41). In D2 mice, the number of macrophages and neutrophils in lung was increased and higher than that of B6 mice (Fig. 6), but it was ineffective to eliminate the bacteria as other bacterial infection (55). This suggests that dysregulation of macrophages and neutrophils and dysregulation of cytokine network in D2 mice cause deficiency to remove invading bacteria. The histopathological result showed that neutrophils infiltration caused damage to the alveolar septa with the production of edema fluid during the infection. The extensive exudate formation within alveoli could further exacerbate the activity of neutrophils and macrophages.

One of the major functions of IL-17A is recruiting neutrophils to site of inflammation (29). The elevation of IL-17A levels during mycoplasma infection in D2 mice, but not B6 mice, is associated with disease pathology, including the recruitment of pulmonary neutrophils (Fig. 6B), which has been also reported in other studies (31). These results suggest that the function of IL-17A in the immune response to mycoplasma may be different based on the genetic background. The elevation of IL-17A exacerbates inflammation by recruiting neutrophils into the airways during the infection (34, 35, 56). It appears that neutrophil recruitment does not induce the recovery of mycoplasmosis, instead worsens the inflammatory response in D2 mice. Reducing inflammatory damage during mycoplasma infection by neutralizing IL-17A (25, 36) could serve as a therapy to reduce lung damage during mycoplasma infection.

The results also found that increase in LC area in MFT was one of the traits that responded to the infection. The immune cells in the LCs consist of mainly T cells and some B cells (15). In normal B6 mice the ratio of LC area to total MFT area was significantly higher than normal D2 mice as shown in previous paper (15) and tended to be increased as increasing the age. However, in this study, it was found that infected D2 mice showed the highest increase in the ratio at 14 d.p.i.. In contrast, the ratio in infected B6 mice was decreased after 7 d.p.i. (Fig. 6). This result was similar to the result in murine auto-immune disease models (16). The increase in the ratio might be caused by over expression of cytokines that induce the proliferation of immune cells in MFT area of D2 mice. For more understanding, cell types in these LC should be identified to elucidate their function that may be involved in the infection. However, it is suspected that these cells may not give any effects or advantages to remove the pathogen but release the cytokine to activate the excessive leukocyte infiltration in the lung. Thus, further

analysis should be needed to identify the type of the inflammatory cells in the LCs of these infected mice.

In summary, it is demonstrated that D2 mice are susceptible to *M. pulmonis*, leading to the development of pneumonia, whereas B6 mice are resistant. The inability to control an effective lung defense might correlate with the lack of initial bactericidal activity in D2 macrophages, indicating that lung macrophages are important factor in the first line of defense against the initial colonization. Additionally, in response to *M. pulmonis* infection, D2 mice are capable of recruiting an increased number of neutrophils to the lung, but fail to protect from the mycoplasma proliferation. These combining factors lead to an increased susceptibility as seen with increased lung colonization, neutrophil recruitment, and severe b.w. loss in D2 mice. This study showed similarity to the bacterial pneumonia and lung injury in humans. These findings could facilitate better understanding in terms of host-pathogen interaction and developing the therapeutics that minimize adverse reactions.

5. SUMMARY

Mycoplasma infections cause respiratory tract damages and atypical pneumonia, resulting in serious problems in humans and animals worldwide. It is well known that laboratory inbred mouse strains show various susceptibility to *M. pulmonis* infection, which causes murine respiratory mycoplasmosis. The progression of murine mycoplasma pneumonia is dependent on immune cells and others. The role of cytokines in immunity are complex, and identifying the network of cytokines produced after infection of mice is essential in dissecting the key cytokine cascades involved in mycoplasma disease pathogenesis. This study aimed to demonstrate the difference in cellular immune responses between resistant strain, C57BL/6NCrSlc (B6) and susceptible strain, DBA/2CrSlc (D2) after challenging *M. pulmonis* infection. To accomplish this, histopathology, cytology, and cytokine analysis were used to monitor changes of immune cells migration and cytokines expression in lungs. D2 mice showed higher amount of bacterial proliferation in lung, higher pulmonary infiltration of immune cells such as neutrophils, macrophages, and lymphocytes, and higher levels of interleukin (IL)-1β, IL-6, IL-17A, and tumor necrosis factor-α in bronchoalveolar lavage fluid than did B6 mice. The results of this study suggest that D2 mice are more susceptible than B6 mice to *M. pulmonis* infection due to a hyper-immune inflammatory response.

CHAPTER 2

QTL analysis of resistance/susceptibility to the *Mycoplasma pulmonis* infection in the mouse

1. INTRODUCTION

QTL mapping locates and estimates the effect of genetic loci that regulate quantitative traits that are complex, continuous and regulated by a group of genes interacting with each other and the environment. Using the inbred mouse strains as a model organism, QTL mapping has become a very important tool for finding genes that regulate complex human diseases, such as mycoplasmosis, inflammatory bowel disease, pneumonia, tuberculosis, diabetes and obesity. In the past two decades, QTL analyses have identified well over 2,000 QTLs associated with such diseases (21, 32) and the genes underlying these QTLs are being identified at a faster pace than ever. The increased role of QTL mapping and favored status of the inbred mouse in that role, are based on the improvement and development of genetic research tools to manipulate the mouse genome.

Most QTLs have been mapped in model organisms such as the mouse and the rat. QTL mapping in humans is difficult, time consuming, expensive, hampered by ethical problems and compromised by populations that are too small, too genetically diverse and subject to uncontrollable environments. Those obstacles are nearly all overcome in the laboratory mouse: the mouse room environment can be tightly controlled; laboratory mice are genetically well defined; mice can produce large populations quickly; the mouse genome can be manipulated in many ways; the laboratory mouse is relatively inexpensive to raise and maintain; QTL mapping projects in the mouse can take less than a year (45); and, most importantly, the biology of the mouse is very similar to that of humans.

That similarity has become evident in the past 15 years as comparative genomics has demonstrated that the location of QTLs in mouse and other model animals can predict the

location of homologous QTLs in humans. It is thought that genes responsible for QTLs are key regulators of interacting biochemical pathways (21, 32) and thus may be potential targets for therapeutic intervention. Because of cross-species concordance, QTLs and their underlying candidate genes can be first identified in mice with cost-effectively, and then the genes can be tested relatively easily in humans and verified in mice.

Mycoplasma species, particularly *M. pulmonis* is an important pathogen in the microbiological test items of SPF animals, because it infects rodents and causes pneumonia. This bacterium is Gram-negative spherical to pear-shaped, facultative anaerobe, lacking a cell wall, and grows on conventional horse serum-yeast extract *Mycoplasma* medium. Animals infected with *M. pulmonis* frequently suffer from lesions in the respiratory tract, as well as the reproductive organs, joints, and brain. The infection can be transmitted by airborne droplet of nasopharyngeal secretion. Mycoplasma infection in laboratory mouse colonies causes severe problems to respiratory tract associated with rhinitis, otitis media, laryngotracheitis, and bronchopneumonia. As a result, *M. pulmonis* can have significant impact on research that uses infected mice through morbidity, mortality and interference with respiratory function (13).

Previous studies with different inbred mouse strains showed various susceptibility to this bacterial infection. For instance, infected B6 mice have bacterial load in their lungs 100,000 times lower than D2 and C3H mice (5) as well as lower gross lung lesions and lung histopathological lesions (10). During thirty years and more, many researchers have tried to elucidate the variation of susceptibility to the *M. pulmonis* infection. However, the genetic loci and genes responsible for the resistance/susceptibility to the infection are still unknown. Therefore, identification of the locus was tried by QTL analysis using F_2 progeny derived from two inbred mouse strains, which show the most clear difference in susceptibility to the infection

such as b.w. loss, lung histopathological lesions, propagation of bacteria in lung cytological changes, cytokine level in BALF, and area of LCs in MFTs as disease-associated phenotypes.

In the Chapter 1 and preliminary study, pathogenicity of the bacteria was examined in B6 and D2 inbred mouse strains. The next step is as follows; select the suitable quantitative trait that can differentiate disease severity between B6 and D2 mice, then a large F_2 population derived from intercross between B6 and D2 mice were challenged with *M. pulmonis*, and QTL analysis was performed to identify genetic loci and genes responsible for susceptibility/resistance to *M. pulmonis* infection. This study expects the elucidation of infection mechanism of *M. pulmonis* and prevention of the infection, if new genes that contribute to the susceptibility/resistance are identified.

2. MATERIALS AND METHODS

2.1. Mice

Based on the previous study (Chapter 1), it has been determined that B6 and D2 mice are resistant and susceptible to *M. pulmonis* infection, respectively. SPF 8-week-old female and male B6 and D2 mice were purchased from Japan SLC (Hamamatsu, Japan) and used as the parental founders of F_2 population. An outcross between the two founders was conducted and subsequently the members of the first generation (F_1 generation) were intercrossed to generate 121 F_2 (B6 x D2) mice. All animals were kept under SPF conditions and infection experiments were conducted in the bio-safety level 3 facilities with sterile food and water *ad libitum*. Animal experimentation was conducted under the AAALAC International-accredited program and animal use protocol was approved by the President of Hokkaido University after review by the Institutional Animal Care and Use Committee (Protocol No. 16-0037).

2.2. Bacteria and experimental infection procedure

The CIEA-NH strain of *M. pulmonis* was kindly provided by Dr. Nobuhito Hayashimoto, Central Institute for Experimental Animals, Japan. Mycoplasma broth was made as follows; 21 g of mycoplasma broth base (BBL Microbiology Systems, Cockeysville, MD, USA), 5 g of D (+) - glucose (Wako Pure Chemical Industries, Ltd., Osaka, Japan), and 20 mg of phenol red (Wako) were dissolved with 750 ml of distilled water, autoclaved for 15 min, allowed to cool, and then 150 ml of heat-inactivated horse serum (GIBCO Laboratories, Grand Island, NY, USA), 100 ml of 25% fresh yeast extracts (Oriental Yeast Co., Ltd., Tokyo, Japan), 10 ml of 2.5% thallium acetate (Wako), and 1,000,000 units of ampicillin sodium salt (Sigma Chemical Company, Saint

Louis, MO, USA) were added. After propagating *M. pulmonis* in the above broth, the stock cultures were divided into 1-ml aliquots and frozen at -80 °C until used. Eight-week-old F_2 (B6 x D2) male and female mice (n = 121) were inoculated intranasally with 6.0×10^5 CFU of *M. pulmonis* in 30 μl of inoculum after anesthetization with inhalation of isoflurane (Escain®;Pfizer Co., Ltd., Tokyo, Japan) followed by intraperitoneal injection of the mixture of 0.75 mg/kg b.w. medetomidine (Domitor®Nippon Zenyaku Kogyo Co., Ltd., Koriyama, Japan), 4.0 mg/kg b.w. midazoram (Dormicum®, Astellas Pharma Inc., Tokyo, Japan), and 5.0 mg/kg b.w. butorphanol (Vetorphale®, Meiji Seika Pharma, Ltd., Tokyo, Japan) (20). The infected dose of inoculum was determined from Chapter 1 that causes the severe pneumonia and 30% b.w. loss in D2 mice, whereas B6 mice exhibited only 5% b.w. loss. Mice were daily observed for clinical signs, b.w., and body temperature. The sampling was performed at 21 d.p.i. after euthanizing mice by inhalation of overdose of isoflurane (Escain®;Pfizer Co., Ltd.,).

2.3. Quantitative culture of *M. pulmonis* in lungs of infected mice

Mice were euthanized at 21 d.p.i.. Lung sampling was done as described in Chapter 1. Briefly, after removed lungs by aseptic technique and homogenized in 1 ml of mycoplasma broth with glass homogenizers (Sankyo Co., Ltd., Tokyo, Japan). Ten-fold serial dilutions were prepared and an aliquot of 10 μl of each dilution was plated onto PPLO agar medium, which was made by dissolving 35 g of PPLO agar (Becton Dickinson and Company, Sparks, MD, USA) with 750 ml of distilled water, autoclaved for 15 min, allowed to cool at 52-54 °C, and then 150 ml of heat-inactivated horse serum (GIBCO), 100 ml of 25% fresh yeast extracts (Oriental Yeast), and 1,000,000 units of ampicillin sodium salt (Sigma) were added. The total number of

CFU per lung from each animal was determined under a stereomicroscope after incubation for 10 days at 37 °C in an incubator with 5% CO_2.

2.4. BALF collection and cytology

Mice were euthanized by inhalation of overdose of isoflurane at 21 d.p.i. and BALF was collected as described in Chapter 1. Briefly, a sterile 20-gauge animal feeding needle (Fuchigami Instruments Co., Ltd., Kyoto, Japan) was inserted through the mouth and larynx into the lumen of the trachea. The lungs were then slowly lavaged *in situ* with three separated 300 μl of sterile PBS, pH 7.2. The BALF was centrifuged at 300 × g at 4 °C for 5 min, and then the supernatants were collected and stored at -80 °C for the cytokine analysis. The cell pellet was suspended in 1.5 ml of distilled water, placed for 10 s, and then added 500 μl of 0.6 M KCl and mixed by inverting. Suspensions were centrifuged at 300 × g at 4 °C for 5 min and the supernatants were discarded. The cell pellets were resuspended by adding 500 μl of sterile saline (0.9% NaCl) with 2.6 mM EDTA and mixed by inverting, and then total count of viable leukocytes was determined by using a heamocytometer (Erma Inc., Tokyo, Japan). To determine differential cell count, 200 μl of the BALF cell suspensions were loaded onto a Shandon™ EZ Single Cytofunnel (Thermo Fisher Scientific, Cheshire, UK) and centrifuged for 10 min at 108 × g. Finally, the slides were dried at room temperature and stained with a Diff-Quick Staining Kit according to the manufacture's protocol.

2.5. Genotyping of microsatellite markers

Extraction of genomic DNA from tail clips was performed by the standard methods. A total of 125 microsatellite markers showing polymorphisms between B6 and D2 mice were used

for genetic study as described previously (42). The map positions of microsatellite loci were based on information from the Mouse Genome Informatics (MGI; http://www.informatics.jax.org), which provides an average interval of approximately 10-20 cM to cover all 19 autosomes and the X chromosome (Table 1). The touchdown PCR was carried out on a Bio-Rad PCR thermal cycler (iCycler, California, USA) with the cycling sequence of 95 °C for 1 min (one cycle), followed by 10 cycles consisting of denaturation at 95 °C for 30 s, primer annealing at 65 °C for 30 s (-2 °C in 2 cycles), and extension at 72 °C for 30 s, then 35 cycles consisting of denaturation at 95 °C for 30 s, primer annealing at 55 °C for 30 s, and extension at 72 °C for 30 s, and final extension at 72 °C for 1 min. PCR mixture and enzymes (Ex*Taq*DNA Polymerase) were purchased from TaKaRa (Otsu, Japan). The amplified samples were electrophoresed with 10-15% polyacrylamide gel (Wako, Osaka, Japan), stained with ethidium bromide, and then photographed under an ultraviolet lamp.

2.6. QTL analysis

One hundred twenty one F_2 (B6 x D2) mice were produced, infected with *M. pulmonis* at 8 weeks old, and measured % b.w. change, CFU of *M. pulmonis* in the lung, and the number of total cells, neutrophils, macrophages, and lymphocytes infiltrated in BALF as QT at 21 d.p.i.. QTL analysis was performed with a Map Manager QTXb20 software program (28). In this program, linkage probability was examined by interval mapping. For each chromosome, the likelihood ratio statistic (LRS) values were calculated by 5,000 random permutations of the trait values relative to genotypes of the maker loci and converted to logarithm of the odds (LOD) score.

2.7. Statistical analysis

The results of the various groups were compared by using ANOVA. Scheffe's post-hoc test was used for multiple comparisons when a significant difference was observed by ANOVA ($P < 0.05$). All values were represented as mean ± SE. Values of $P \leq 0.05$ were considered statistical significance.

3. RESULTS

3.1. Susceptibility to *M. pulmonis* infection in F_2 (B6 x D2) progeny

Experiments in Chapter 1 established that the intranasal inoculation of 6.0×10^5 CFU of *M. pulmonis* in 30 μl of inoculum caused severe pneumonia and 30% b.w. loss in D2 mice, whereas B6 mice exhibited only 5% b.w. loss. To analyze the potential contribution of genetic factors to *M. pulmonis* infection, the F_1 population and subsequent 121 F_2 mice were generated by reciprocal mating of resistant B6 and susceptible D2 mice. The entire F_2 population was infected as described above and b.w. change of each mouse was daily recorded until 21 d.p.i.. Total cell count, differential cell count, and CFU/lung were also assessed by cytology and culture in F_2 mice. F_2 progeny showed a b.w. loss, which was significantly lower than the susceptible strain D2, but significantly higher than the B6 parental strain (Fig. 14).

3.2. QTL analysis

To dissect genetic factors regulating susceptibility or resistance to the *M. pulmonis* infection between B6 and D2 mice, QTL analysis was performed. The 121 F_2 mice were genotyped using 125 microsatellite markers. % b.w. change, CFU of *M. pulmonis* in the lung, and the number of total cells, neutrophils, macrophages, and lymphocytes infiltrated in BALF were selected as QTs. Detected QTLs were different each other depending on QTs used (Figs. 12 and 13). Only when b.w. change was used as QT, a significant QTL was obtained on Chr 4 (Fig. 12). The QTL on Chr 4 explained 13% of the total variance of % b.w. change in the F_2 population. The peak signal for this QTL was at *D4Mit42* located at 151.6 Mbp with 3.6 LOD score, which mapped to the distal region of Chr 4, residing within 17.1 Mbp between *D4Mit54*

and *D4Mit256*. The mapped QTL on Chr 4 was named *Mpil1* for *M. pulmonis* infection locus 1. These data suggest that the difference in each phenotype between infected B6 and D2 is attributed to different genetic factors.

3.3. Identification of candidate genes in Chr 4

The positions of the closest markers flanking the peak on Chr 4 were used to define the boundaries of this interval on the mouse genome assembly and searched for genes that might be involved in the progression of *M. pulmonis* infection based on their expression profiles in the literature and public databases. A total of 487 genes within *Mpil1* interval were identified from the public database, MGI, as described in materials and methods and classified as protein coding genes (n = 247), non-coding RNA genes (n = 212) and unclassified genes (n = 28). To prioritize these genes, MGI database was used by based the search on different keywords (Lung, Infection, Respiratory AND Infection) and gene ontology terms (Immune AND Response, Cytokines, Chemotaxis). The candidate genes in Table 2 are those reviewed by the literature research as having a putative role in host defense to infection. In particular, the most promising candidate genes (*Tnfrsf1b, Trp73*) were those involved in pathogen sensing, immune cells recruitment, and inflammatory process in respiratory system. Prioritization of results depends on the adopted criteria for the bioinformatics analysis and on the bioinformatics tool itself. Therefore, it cannot be excluded that other possible candidate genes presented in the list could somehow play a role in *M. pulmonis* infection.

Table 1. Microsatellite markers used for the QTL analysis

Microsatellite Markers	Mbp	Microsatellite Markers	Mbp	Microsatellite Markers	Mbp	Microsatellite Markers	Mbp	Microsatellite Markers	Mbp
D1Mit427	4	*D4Mit139*	55	*D7Mit333*	137	*D11Mit199*	101	*D16Mit182*	5
D1Mit70	32	*D4Mit152*	83	*D8Mit155*	4	*D11Mit48*	118	*D16Mit59*	38
D1Mit324	58	*D4Mit308*	124	*D8Mit4*	32	*D12Mit182*	10	*D16Mit171*	56
D1Mit415	86	*D4Mit54*	137	*D8Mit100*	56	*D12Mit172*	46	*D16Mit140*	70
D1Mit191	120	*D4Mit42*	151	*D8Mit234*	82	*D12Mit36*	60	*D16Mit152*	85
D1Mit14	156	*D5Mit345*	4	*D8Mit242*	101	*D12Mit5*	80	*D16Mit106*	97
D1Mit291	184	*D5Mit180*	24	*D8Mit200*	114	*D12Mit101*	102	*D17Mit113*	11
D1Mit155	194	*D5Mit108*	43	*D8Mit56*	129	*D12Mit150*	115	*D17Mit198*	27
D2Mit175	3	*D5Mit258*	66	*D9mit219*	13	*D13Mit57*	16	*D17Mit139*	52
D2Mit296	31	*D5Mit357*	77	*D9Mit90*	32	*D13Mit60*	35	*D17Mit218*	71
D2Mit91	66	*D5Mit208*	100	*D9Mit4*	52	*D13Mit248*	52	*D17Mit221*	90
D2Mit66	84	*D5Mit188*	117	*D9Mit302*	67	*D13Mit9*	81	*D18Mit66*	3
D2Mit62	118	*D5Mit370*	126	*D9Mit133*	84	*D13Mit35*	119	*D18Mit132*	21
D2Mit286	154	*D5Mit222*	142	*D9Mit355*	98	*D14Mit10*	12	*D18Mit17*	39
D2Mit200	179	*D6Mit86*	4	*D9Mit18*	120	*D14Mit120*	36	*D18Mit124*	57
D3Mit164	7	*D6Mit159*	29	*D10Mit248*	14	*D14Mit102*	65	*D18Mit7*	76
D3Mit268	28	*D6Mit74*	48	*D10Mit61*	66	*D14Mit225*	74	*D19Mit69*	13
D3Mit182	50	*D6Mit188*	75	*D10Mit186*	75	*D14Mit7*	90	*D19Mit80*	23
D3Mit241	66	*D6Mit104*	110	*D10Mit134*	104	*D14Mit170*	106	*D19Mit119*	41
D3Mit28	90	*D6Mit15*	146	*D10Mit297*	125	*D14Mit266*	121	*D19Mit33*	56
D3Mit346	116	*D7Mit178*	3	*D11Mit226*	8	*D15Mit12*	3	*DXMit89*	10
D3Mit14	132	*D7Mit114*	26	*D11Mit229*	25	*D15Mit5*	43	*DXMit166*	51
D3Mit129	156	*D7Mit82*	51	*D11Mit21*	44	*D15Mit156*	71	*DXMit25*	71
D4Mit235	8	*D7Mit318*	73	*D11Mit4*	68	*D15Mit159*	87	*DXMit130*	133
D4Mit172	34	*D7Mit66*	119	*D11Mit212*	88	*D15Mit161*	97	*DXMit186*	165

Table 2. The list of the most promising candidate genes identified in the *Mpil1* locus on Chr 4

Gene symbol	Gene description	Mbp
D4Mit54	**Flanking marker**	**137.8**
Crocc	Ciliary rootlet coiled-coil, rootletin	141.0
Cplane2	Ciliogenesis and planar polarity effector 2	141.2
Prdm2	PR domain containing 2, with ZNF domain	143.1
Pdpn	Podoplanin	143.2
Tnfrsf1b	Tumor necrosis factor receptor superfamily, member 1b	145.2
Gm572	Predicted gene 572	148.6
Kif1b	Kinesin family member 1B	149.1
Errfi1	ERBB receptor feedback inhibitor 1	150.8
D4Mit42	**Significant locus**	**151.5**
Trp73	Transformation related protein 73	154.0
Prdm16	PR domain containing 16	154.3

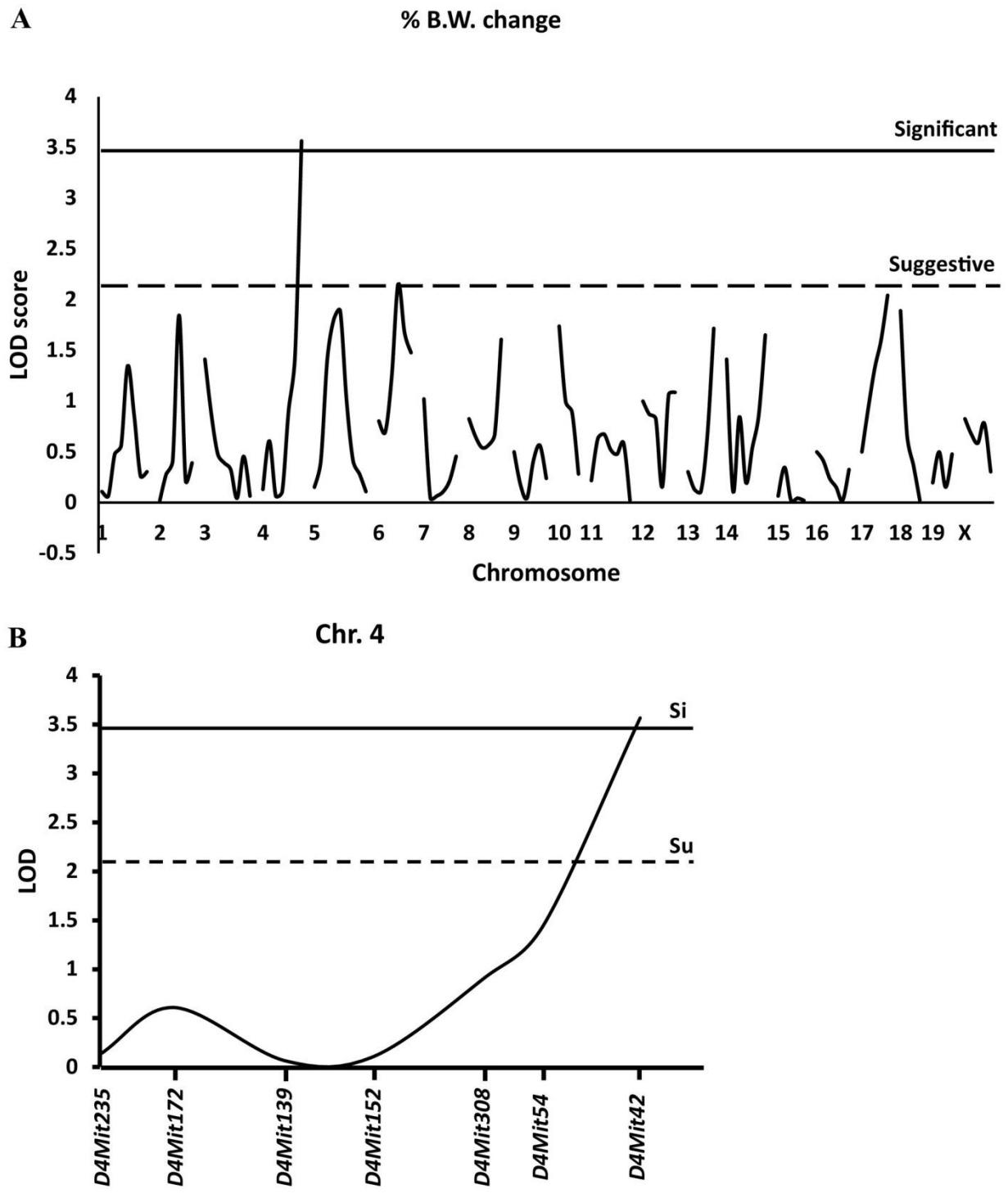

Fig. 12. QTL scan showing LOD score and genome positions associated with the % b.w. change after *M. pulmonis* infection. (A) The x and y axes show Chr number and LOD score,

respectively. The horizontal lines across the plot indicate two confidence thresholds calculated at 5% (thick, significant) and 63% (dotted, suggestive) level of significance. One significant QTL ($P = 0.00027$) was detected at 151.6 Mbp on Chr 4 with 3.6 LOD score and one suggestive QTL ($P = 0.00713$) was detected at 75.4 Mbp on Chr 6 with 2.2 LOD score. (B) Enlarged figure for Chr 4. The x and y axes show microsatellite marker positions and LOD score, respectively.

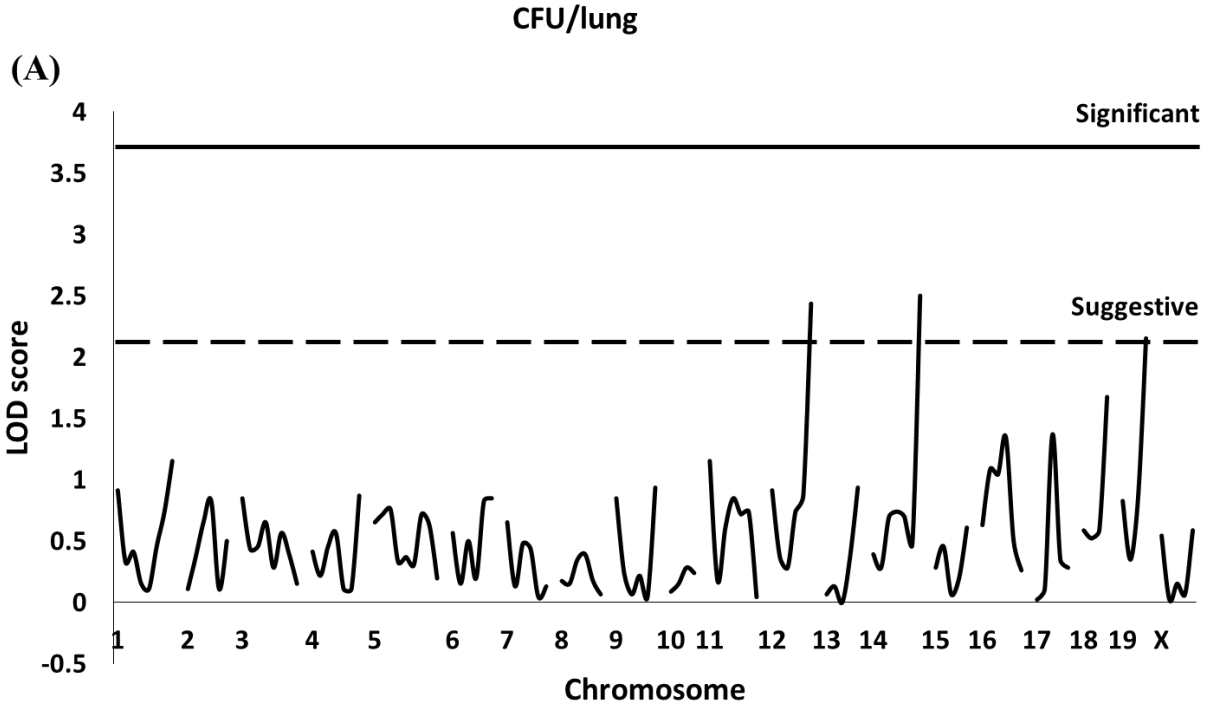
CFU/lung
(A)
Significant
Suggestive
LOD score
4
3.5
3
2.5
2
1.5
1
0.5
0
-0.5
1 2 3 4 5 6 7 8 9 10 11 12 13 14 15 16 17 18 19 X
Chromosome

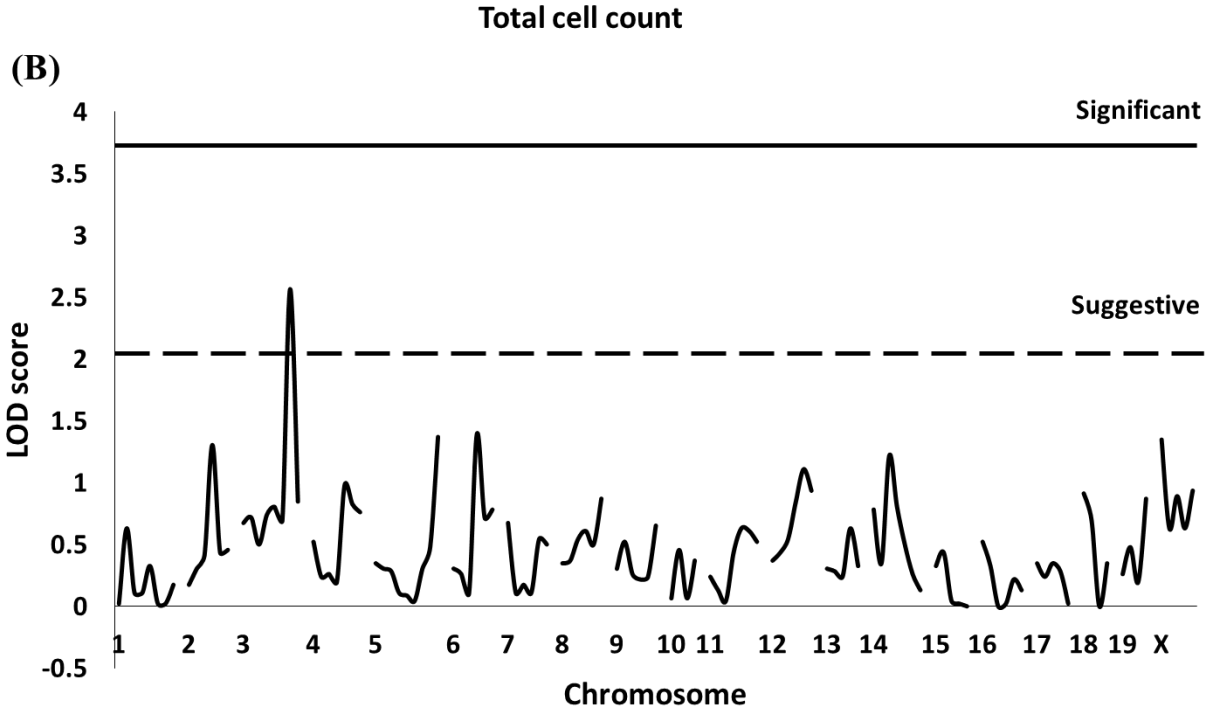
Total cell count
(B)
Significant
Suggestive
LOD score
4
3.5
3
2.5
2
1.5
1
0.5
0
-0.5
1 2 3 4 5 6 7 8 9 10 11 12 13 14 15 16 17 18 19 X
Chromosome

% Neutrophils

(C)

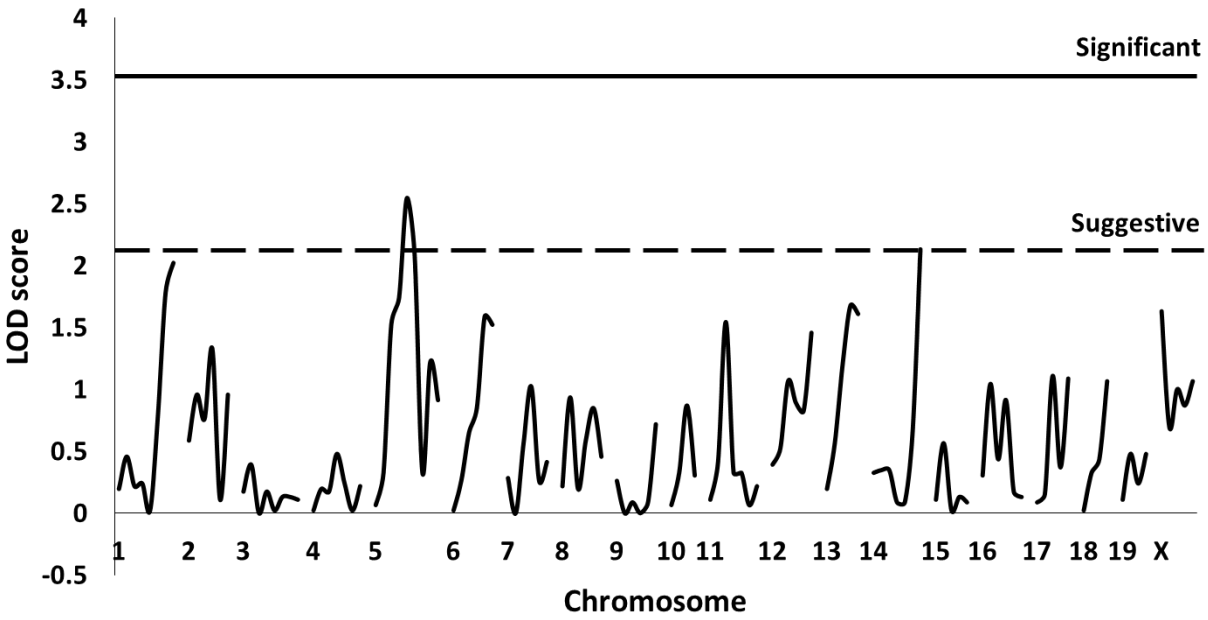

% Macrophages

(D)

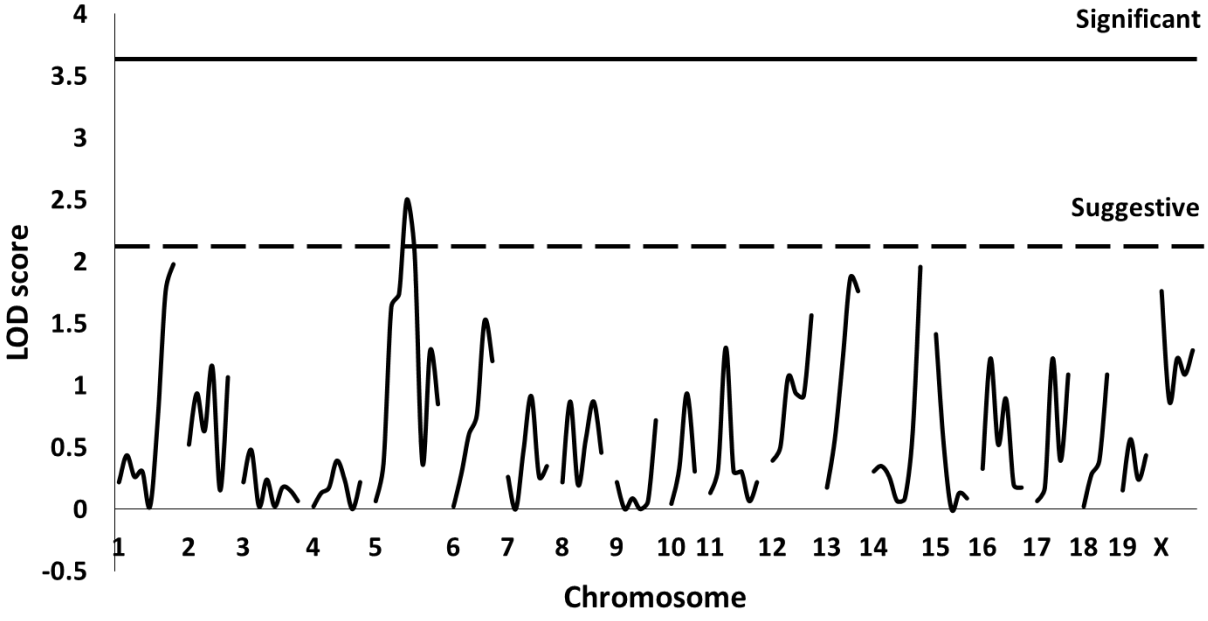

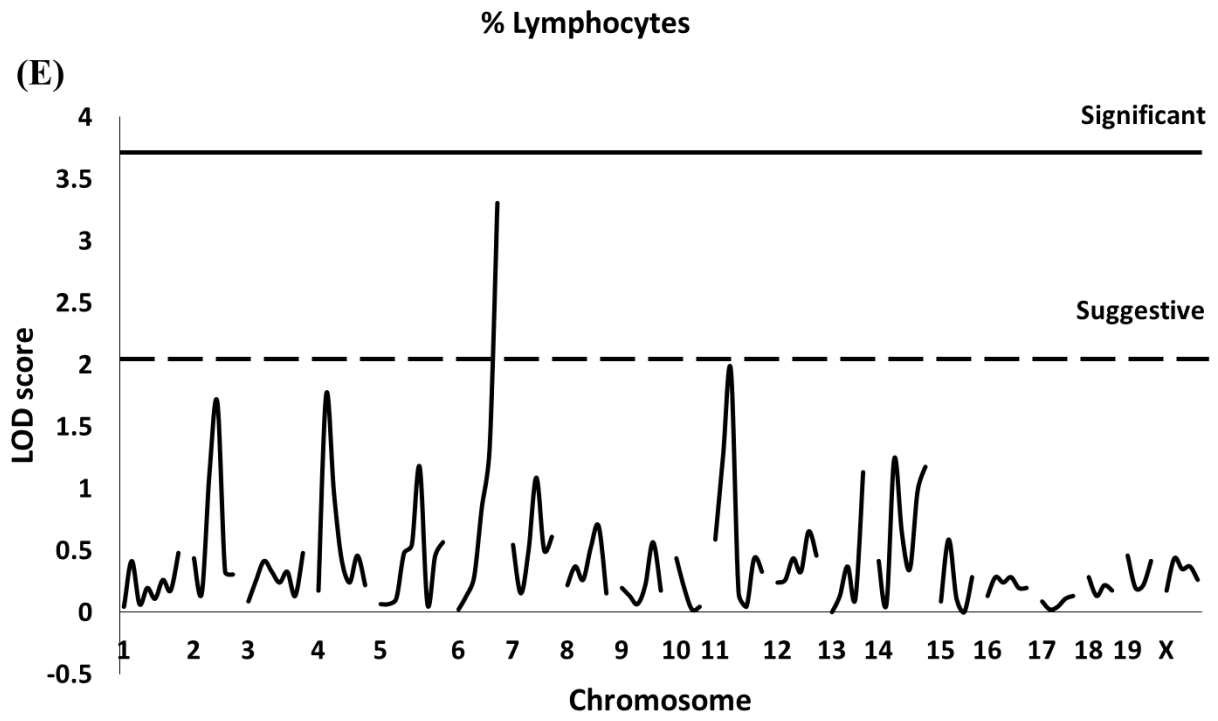

Fig. 13. QTL scan showing LOD score and genome positions associated with the designed QTs after *M. pulmonis* infection. The x and y axes show Chr number and LOD score, respectively. The horizontal lines across the plot indicate two confidence thresholds calculated at 5% (thick, significant) and 63% (dotted, suggestive) level of significance. (A) QTL scan showing LOD score and genome positions associated with the CFU/lung after *M. pulmonis* infection. Three suggestive QTL (P = 0.0038, 0.00317, and 0.0072) were detected at 115.9, 121.0, and 56.1 Mbp on Chr 12, 14, and 19 with 2.4, 2.5, and 2.2 LOD score, respectively. (B) QTL scan showing LOD score and genome positions associated with the total cell count after *M. pulmonis* infection. One suggestive QTL (P = 0.0028) was detected at 132 Mbp on Chr 3 with 2.6 LOD score. (C) QTL scan showing LOD score and genome positions associated with the % of neutrophils after *M. pulmonis* infection. Two suggestive QTL (P = 0.00288, and 0.00743) were detected at 77.1, and 121.0 Mbp on Chr 5, and 14 with 2.5, and 2.1 LOD score, respectively. (D) QTL scan

showing LOD score and genome positions associated with the % of macrophages after *M. pulmonis* infection. One suggestive QTL (P = 0.00324) was detected at 77.1 Mbp on Chr 5 with 2.5 LOD score. (E) QTL scan showing LOD score and genome positions associated with the % of lymphocytes after *M. pulmonis* infection. One suggestive QTL (P = 0.0005) was detected at 146.4 Mbp on Chr 6 with 3.3 LOD score.

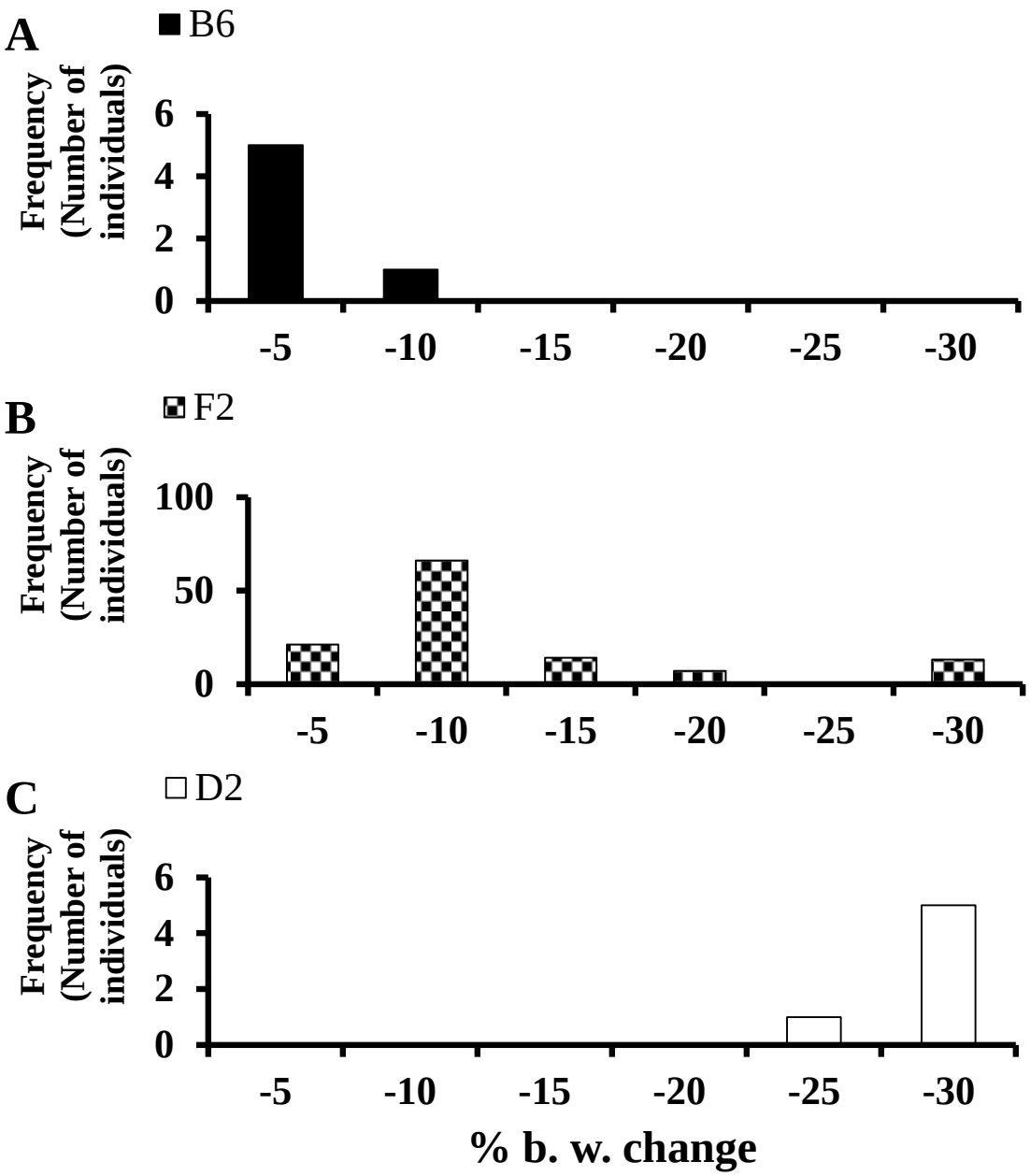

Fig. 14. Histogram of % b.w. change of B6, D2 and F_2 population after *M. pulmonis* infection. A, B6 (n = 6), B, F_2 (n = 121), and C, D2 (n = 6) mice were intranasally inoculated with a dose of 6.0×10^{-5} CFU of *M. pulmonis*, and recorded for b.w. change up to 21 d.p.i..

4. DISCUSSION

Phenotypic variations of host response to *M. pulmonis* infection have been demonstrated in several inbred mouse strains (4, 5, 46) and autoimmune disease mouse (54). In Chapter 1, it was shown that classical inbred strains of mice manifested an extreme response, highly resistant or highly susceptible to *M. pulmonis* infection. In particular, the risk of severe b.w. loss, high bacterial propagation in lung, high inflammatory cells infiltration and high cytokines level in D2 mice was observed after exposure to *M. pulmonis*, while B6 mice showed milder clinical symptoms associated to higher resolution of the infection. However, the genetic component of this trait is still poorly understood. In this study, a genetic determinant of susceptibility to *M. pulmonis* infection was investigated. First, an informative F_2 population was generated by crossing the resistant B6 and susceptible D2 mice. Next, this F_2 population was scored for % b.w. change as the main phenotypic trait associated with disease progression, and subsequently used for QTL analysis. The *M. pulmonis* dose for inoculation of the newly generated population was selected according to the most deviant differences in % b.w. change between parental strains. The F_2 population showed a wide range of responses in terms of % b.w. change compared to the parental strains. For this study, *M. pulmonis* isolates sampled from wild mouse showed a clinical sign of the disease. Although the *M. pulmonis* strain was selected on the basis of its similarity to environmental strains, including genotypic and phenotypic features, it is possible that this particular strain may affect several physiological parameters and subsequent analysis.

Genetic linkage approach was successful in identifying for the first time the *Mpil1* locus, on murine Chr 4, linked to susceptibility to *M. pulmonis* infection with 95% significance ($P < 0.05$). Here, the gene prioritization approach was used to rank genes involved in the

susceptibility to *M. pulmonis* infection. The most promising candidate genes included in the *Mpil1* locus, namely *Crocc, Cplane2, Prdm2, Pdpn, Tnfrsf1b, Gm572, Kif1b, Errfi1, Trp73 and Prdm16*, are mainly involved in pathogen sensing, immune cells recruitment, and inflammatory process in respiratory system.

Finally, QTL analysis was performed to dissect genetic factors controlling the difference in infected phenotypes and obtained many loci. However, detected QTL responsible for each phenotype was different each other (Figs. 12 and 13). This result suggests that the difference in each phenotype is expressed under the control of respective genetic factor, indicating that many different genetic factors are present between B6 and D2 mice. However, only one significant QTL was detected on Chr 4. A significant QTL have been obtained on Chr 4, when QTL analysis was performed for resistance or susceptibility to Sendai virus infection using b.w. change as QT between B6 and D2 mice (42). Although peak position of the QTL is slightly different, it is quite interesting to hypothesize that some genetic factors on Chr 4 may contribute to resistance or susceptibility to pathogens causing pneumonia. In addition, a suggestive QTL have been obtained on Chr 6, which was reported that relate to production of adipose tissue and b.w. control (44).

In summary, promising candidates for the genetic basis of host susceptibility to *M. pulmonis* infection are suggested. In addition to a better understanding of host pathogen interactions, the characterization of these genes may have significant implications for the discovery of novel possible therapeutic targets and/or prognostic biomarkers complementing human studies.

5. SUMMARY

Genetics factor plays a key role in host response, disease severity, and ultimate outcome of the infection with *M. pulmonis* in rodents. In the mouse, D2 strain is very susceptible to *M. pulmonis* infection, while the B6 strain is resistant. In D2 mice, a heavier bacterial burden causes a unique phenotype that includes very severe and fatal pulmonary disease with extensive exudation of macrophages and neutrophils and tissue necrosis, as opposed to slower progressive pulmonary disease characterized by the accumulation of epithelioid macrophages with protective immune and inflammatory responses in B6 mice. To identify the genes responsible for the differences in host response to *M. pulmonis* in these two strains, 121 F_2 (B6 X D2) crosses were infected intranasally with *M. pulmonis* and % b.w. change, CFU of *M. pulmonis* in the lung, and number of total cells, neutrophils, macrophages, and lymphocytes infiltrated in bronchoalveolar lavage fluid were used as QTs in a whole genome scan. Quantitative trait locus (QTL) analysis showed that the susceptibility was controlled by multi-genic loci. However, % b.w. change was used as a QT, QTL analysis identified one significant linkage on the distal portion of chromosome (Chr) 4 (*D4Mit42*, 3.6 LOD) and one suggestive linkage on Chr 6 (*D6Mit188*, 2.2 LOD) that totally account for approximately 21% of the phenotypic variance. These novel loci provide the basis for the evaluation of a possible association of the corresponding syntenic chromosomal regions in humans with respect to the susceptibility to mycoplasmosis.

CONCLUSION

Mycoplasma infections cause respiratory tract damages and atypical pneumonia, resulting in serious problems in humans and animals worldwide. *Mycoplasma* species, particularly *Mycoplasma pulmonis (M. pulmonis)* is an important pathogen involved in microbiological test items of specific pathogen-free rodents, because it causes pneumonia after infection in rodents. As a result, *M. pulmonis* has significant impact on research using rodents. Previous studies with different inbred mouse strains showed various susceptibilities to this bacterial infection. For instance, infected C57BL/6 (B6) mice have bacterial load in their lungs 100,000 times lower than DBA/2 (D2) mice as well as lower gross lung lesions and lung histopathological lesions. However, the profiling of cellular immune responses and the genetic loci or genes responsible for the resistance/susceptibility to the infection are still little known.

In Chapter 1, the cellular immune response was examined by using two inbred mouse strains, B6 (resistant) and D2 (susceptible), to exhibit the profiling of the infection by observing disease-associated phenotypes such as lung histopathological lesions, propagation of bacteria in lung, lung cytological change, cytokine levels in BALF, and areas of lymphoid clusters (LCs) in mediastinal fat tissues (MFTs). D2 mice constantly had much greater number of colony-forming unit (CFU) of *M. pulmonis* in their lung, greater severity of lung lesions, higher pulmonary infiltration of immune cells, and higher levels of cytokines in BALF. This study first examined and complied the cellular immune responses from *M. pulmonis* infection in B6 and D2 mice. These results suggest that D2 mice are more susceptible than B6 mice to *M. pulmonis* infection due to a hyper-immune inflammatory response.

In Chapter 2, quantitative trait locus (QTL) analysis was performed using the infected phenotypes (in Chapter 1) that showed the difference between infected B6 and D2 mice as quantitative traits (QTs) to dissect genetic factors regulating the difference between these two inbred strains. Detected QTLs were different each other depending on QTs used. These data suggest that the difference in each phenotype between infected B6 and D2 is attributed to different genetic factors. However, only when body weight change was used as a QT, a significant QTL was detected on chromosome (Chr) 4. The peak signal for this QTL was at *D4Mit42* located at 151.6 Mbp with 3.6 LOD score, which mapped to the distal region of Chr 4, residing within 17.1 Mbp between *D4Mit54* and *D4Mit256*. This region included some candidate genes that might be involved in *M. pulmonis* infection. Further study of this locus may provide insights into therapeutic strategy for murine respiratory mycoplasmosis.

In conclusion, from this study, the profiling of cellular immune response to *M. pulmonis* infection in B6 and D2 mice was established. These data provided the better understanding of immune systems that response to the infection and would benefit to the identification of genetic loci and genes responsible for the host defense to the *M. pulmonis* infection. Moreover, the result may be extrapolated to mycoplasmosis in other animals including human.

REFERENCES

1. Boettger, C.M., Dohms, J.E., 2006. Separating *Mycoplasma gallisepticum* field strains from nonpathogenic avian mycoplasmas. Avian Dis. 50, 605–607.
2. Calcutt, M.J., Lysnyansky, I., Sachse, K., Fox, L.K., Nicholas, R.A.J., Ayling, R.D., 2018. Gap analysis of *Mycoplasma bovis* disease, diagnosis and control: an aid to identify future development requirements. Transbound. Emerg. Dis. 65, 91–109.
3. Cardona, P.J., Gordillo, S., Díaz, J., Tapia, G., Amat, I., Pallarés, Á., Vilaplana, C., Ariza,A., Ausina, V., 2003. Widespread bronchogenic dissemination makes DBA/2 mice more susceptible than C57BL/6 mice to experimental aerosol infection with *Mycobacterium tuberculosis*. Infect. Immun. 71, 5845–5854.
4. Cartner, S.C., Simecka, J.W., Lindsey, J.R., Cassell, G.H., Davis, J.K., 1995. Chronic respiratory mycoplasmosis in C3H/HeN and C57BL/6N mice: lesion severity and antibody response. Infect. Immun. 63, 4138–4142.
5. Cartner, S.C., Simecka, J.W., Briles, D.E., Cassell, G.H., Lindsey, J.R., 1996. Resistance to mycoplasmal lung disease in mice is a complex genetic trait. Infect. Immun. 64, 5326–5331.
6. Ceola, C.F., Sampaio, J., Blatt, S.L., Cordova, C.M.M., 2016. Mycoplasma infection and inflammatory effects on laboratory rats bred for experimental research. Rev. Pan-Amaz Saude 7, 59–66.
7. Chawla, S., Jena, S., Venkatsan, B., Mahara, K., Sahu, N., 2017. Clinical, pathological, and molecular investigation of *Mycoplasma pulmonis*-induced murine respiratory mycoplasmosis in a rat (*Rattus norvegicus*) colony. Vet. World 10, 1378–1382.

8. Chen, J., Liao, M.Y., Gao, X.L., Zhong, Q., Tang, T.T., Yu, X., Liao, Y.H., Cheng, X., 2013. IL-17A induces pro-inflammatory cytokines production in macrophages via MAPKinases, NF-κB and AP-1. Cell. Physiol. Biochem. 32, 1265–1274.
9. Daubeuf, F., Frossard, N., 2012. Performing bronchoalveolar lavage in the mouse. Curr. Protoc. Mouse Biol. 2, 167–175.
10. Davidson, M.K., Lindsey, J.R., Parker, R.F., Tully, J.G., Cassell, G.H., 1988. Differences in virulence for mice among strains of *Mycoplasma pulmonis*. Infect. Immun. 56, 2156–2162.
11. Davis, J.K., Parker, R.F., White, H., Dziedzic, D., Taylor, G., Davidson, M.K., Cox, N.R., Cassell, G.H., 1985. Strain differences in susceptibility to murine respiratory mycoplasmosis in C57BL/6 and C3H/HeN mice. Infect. Immun. 50, 647–654.
12. Diaz, M.H., Benitez, A.J., Winchell, J.M., 2015. Investigations of *Mycoplasma pneumoniae* infections in the United States: trends in molecular typing and macrolide resistance from 2006 to 2013. J. Clin. Microbiol. 53, 124–130.
13. Dobbs, N.A., Zhou, X., Pulse, M., Hodge, L.M., Schoeb, T.R., Simecka, J.W., 2014. Antigen-pulsed bone marrow-derived and pulmonary dendritic cells promote Th2 cell responses and immunopathology in lungs during the pathogenesis of murine *Mycoplasma pneumonia*. J. Immunol. 193, 1353–1363.
14. Elewa, Y.H., Bareedy, M.H., Abuel-Atta, A.A., Ichii, O., Otsuka, S., Kanazawa, T., Lee, S.H., Hashimoto, Y., Kon, Y., 2010. Structural characteristics of goat (*Capra hircus*) parotid salivary glands. Jpn. J. Vet. Res. 58, 121–135.
15. Elewa, Y.H., Ichii, O., Otsuka, S., Hashimoto, Y., Kon, Y., 2014. Characterization of mouse mediastinal fat-associated lymphoid clusters. Cell Tissue Res. 357, 731–741.

16. Elewa, Y.H., Ichii, O., Kon, Y., 2015. Comparative analysis of mediastinal fat-associated lymphoid cluster development and lung cellular infiltration in murine autoimmune disease models and the corresponding normal control strains. Immunology 147, 30–40.
17. Ferreira, J.B., Yamaguti, M., Marques, L.M., Oliveira, R.C., Neto, R.L., Buzinhani, M., Timenetsky, J., 2008. Detection of *Mycoplasma pulmonis* in laboratory rats and technicians. Zoonoses Public Health 55, 229–234.
18. Harasawa, R., Mizusawa, H., Fujii, M., Yamamoto, J., Mukai, H., Uemori, T., Asada, K., Kato, I., 2005. Rapid detection and differentiation of the major mycoplasma contaminants in cell cultures using real-time PCR with SYBR green I and melting curve analysis. Microbiol. Immunol. 49, 859–863.
19. Hickman-Davis, J.M., Michalek, S.M., Gibbs-Erwin, J., Lindsey, J.R., 1997. Depletion of alveolar macrophages exacerbates respiratory mycoplasmosis in mycoplasma-resistant C57BL mice but not mycoplasma-susceptible C3H mice. Infect. Immun. 65, 2278–2282.
20. Kawai, S., Takagi, Y., Kaneko, S., Kurosawa, T., 2011. Effect of three types of mixed anesthetic agents alternate to ketamine in mice. Exp. Anim. 60, 481–487.
21. Korstanje, R., Paigen, B., 2002. From QTL to gene: the harvest begins. Nat. Genet. 31, 235–236.
22. Lai, W.C., Pakes, S.P., Bennett, M., 1996. Natural resistance to *Mycoplasma pulmonis* infection in mice: host resistance gene(s) map to chromosome 4. Nat. Immun. 15, 241–248.
23. Lai, W.C., Linton, G., Bennett, M., Pakes, S.P., 1993. Genetic control of resistance to *Mycoplasma pulmonis* infection in mice. Infect. Immun. 61, 4615–4621.

24. Lan, Y., Chen, Z., Yang, D., Wang, X., Wang, Y., Xu, Y., Tang, L., 2016. Altered cytokine levels in bronchoalveolar lavage fluids from patients with *Mycoplasma pneumonia* infection. Int. J. Clin. Exp. Med. 9, 16548–16557.
25. Liu, L., Lu, J., Allan, B.W., Tang, Y., Tetreault, J., Chow, C.K., Barmettler, B., Nelson, J.,Bina, H., Huang, L., Wroblewski, V.J., Kikly, K., 2016. Generation and characterization of ixekizumab, a humanized monoclonal antibody that neutralizes interleukin-17A. J. Inflamm. Res. 9, 39–50.
26. Loganbill, J.K., Wagner, A.M., Besselsen, D.G., 2005. Detection of *Mycoplasma pulmonis* by fluorogenic nuclease polymerase chain reaction analysis. Comp. Med. 55, 419–424.
27. Luehrs, A., Siegenthaler, S., Grützner, N., Beilage, E.G., Kuhnert, P., Nathues, H., 2017. Occurrence of mycoplasma hyorhinis infections in fattening pigs and association with clinical signs and pathological lesions of enzootic pneumonia. Vet. Microbiol. 203, 1–5.
28. Manly, K.F., Cudmore Jr., R.H., Meer, J.M., 2001. Map manager QTX, cross-platform software for genetic mapping. Mamm. Genome 12, 930–932.
29. Michel, M.L., Keller, A.C., Paget, C., Fujio, M., Trottein, F., Savage, P.B., Wong, C.H., Schneider, E., Dy, M., Leite-de-Moraes, M.C., 2007. Identification of an IL-17-producing NK1.1 (neg) iNKT cell population involved in airway neutrophilia. J. Exp. Med. 204, 995–1001.
30. Miossec, P., Korn, T., Kuchroo, V.K., 2009. Interleukin-17 and type 17 helper T cells. N. Engl. J. Med. 361, 888–898.

31. Mize, M.T., Sun, X.L., Simecka, J.W., 2018. Interleukin-17A exacerbates disease severity in BALB/c mice susceptible to lung infection with *Mycoplasma pulmonis*. Infect. Immun. 86, e00292–18.

32. Moore, K.J., Nagle, D.L., 2000. Complex trait analysis in the mouse: The strengths, the limitations and the promise yet to come. Annu. Rev. Genet. 34, 653–686.

33. Nicolson, G.L., Nasralla, M.Y., Nicolson, N.L., 1999. The pathogenesis and treatment of mycoplasmal infections. Antimicrobics and Infectious Diseases Newsletter (Elsevier Science). 17, 81–88.

34. Okamoto Yoshida, Y., Umemura, M., Yahagi, A., O'Brien, R.L., Ikuta, K., Kishihara, K.,Hara, H., Nakae, S., Iwakura, Y., Matsuzaki, G., 2010. Essential role of IL-17A in the formation of a mycobacterial infection-induced granuloma in the lung. J. Immunol.184, 4414–4422.

35. Park, H., Li, Z., Yang, X.O., Chang, S.H., Nurieva, R., Wang, Y.H., Wang, Y., Hood, L., Zhu,Z., Tian, Q., Dong, C., 2005. A distinct lineage of CD4 T cells regulates tissue inflammation by producing interleukin 17. Nat. Immun. 6, 1133–1141.

36. Patel, D.D., Lee, D.M., Kolbinger, F., Antoni, C., 2013. Effect of IL-17A blockade with secukinumab in autoimmune diseases. Ann. Rheum. Dis. 72, ii116–123.

37. Pereyre, S., Goret, J., Bébéar, C., 2016. *Mycoplasma pneumoniae*: current knowledge on macrolide resistance and treatment. Front. Microbiol. 7, 974.

38. Pica, N., Iyer, A., Ramos, I., Bouvier, N.M., Fernandez-Sesma, A., García-Sastre, A., Lowen, A.C., Palese, P., Steel, J., 2011. The DBA.2 mouse is susceptible to disease following infection with a broad, but limited, range of influenza a and B viruses. J. Virol. 85, 12825–12829.

39. Razin, S., 1996. Mycoplasmas, in: Baron, S. (Eds), Medical Microbiology, 4th ed. University of Texas Medical Branch at Galveston, Galveston, chapter 37.

40. Rollins, S., Colby, T., Clayton, F., 1986. Open lung biopsy in *Mycoplasma pneumoniae* pneumonia. Arch. Pathol. Lab. Med. 110, 34–41.

41. Sahoo, M., Ceballos-Olvera, I., del Barrio, L., Re, F., 2011. Role of the inflammasome, IL-1β, and IL-18 in bacterial infections. Sci. World J. 11, 2037–2050.

42. Simon, A.Y., Moritoh, K., Torigoe, D., Asano, A., Sasaki, N., Agui, T., 2009. Multigenic control of resistance to Sendai virus infection in mice. Infect. Genet. Evol. 9, 1253–1259.

43. Simon, A.Y., Sasaki, N., Ichii, O., Kajino, K., Kon, Y., Agui, T., 2011. Distinctive and critical roles for cellular immunity and immune-inflammatory response in the immunopathology of Sendai virus infection in mice. Microbes Infect. 13, 783–797.

44. Stewart, T.P., Mao, X., Aqqad, M.N., Uffort, D., Dillon, K.D., Saxton, A.M., Kim, J.H., 2012. Subcongenic analysis of *tabw2* obesity QTL on mouse chromosome 6. BMC Genet. 13, 81.

45. Sugiyama, F., Churchill, G.A., Higgins, D.C., Johns, C., Makaritsis, K.P., Gavras, H., Paigen, B., 2001. Concordance of murine quantitative trait loci for salt-induced hypertension with rat and human loci. Genomics. 71, 70–77.

46. Sun, X., Jones, H.P., Hodge, L.M., Simecka, J.W., 2006. Cytokine and chemokine transcription profile during *Mycoplasma pulmonis* infection in susceptible and resistant strains of mice: macrophage inflammatory protein 1β (CCL4) and monocyte chemoattractant protein 2 (CCL8) and accumulation of $CCR5^+$ Th cells. Infect. Immun.74, 5943–5954.

47. Sung, H., Kang, S.H., Bae, Y.J., Hong, J.T., Chung, Y.B., Lee, C.K., Song, S., 2006. PCR-based detection of mycoplasma species. J. Microbiol. 44, 42–49.

48. Szczepanek, S.M., Majumder, S., Sheppard, E.S., Liao, X., Rood, D., Tulman, E.R., Wyand, S., Krause, D.C., Silbart, L.K., Geary, S.J., 2012. Vaccination of BALB/c mice with an avirulent *Mycoplasma pneumoniae* P30 mutant results in disease exacerbation upon challenge with a virulent strain. Infect. Immun. 80, 1007–1014.

49. Takahashi-Omoe, H., Omoe, K., Matsushita, S., Kobayashi, H., Yamamoto, K., 2004. Polymerase chain reaction with a primer pair in the 16S-23S rRNA spacer region for detection of *Mycoplasma pulmonis* in clinical isolates. Comp. Immunol. Microbiol. Infect. Dis. 27, 117–128.

50. Vogels, M.T., Mensink, E.J., Ye, K., Boerman, O.C., Verschueren, C.M., Dinarello, C.A., van der Meer, J.W., 1994. Differential gene expression for IL-1 receptor antagonist, IL-1, and TNF receptors and IL-1 and TNF synthesis may explain IL-1-induced resistance to infection. J. Immunol. 153, 5580–5772.

51. Vogels, M.T., Eling, M.T., Otten, A., van der Meer, J.W., 1995. Interleukin-1 (IL-1)-induced resistance to bacterial infection: role of the type I IL-1 receptor. Antimicrob. Agents Chemother. 39, 1744–1747.

52. Waites, K.B., Talkington, D.F., 2004. *Mycoplasma pneumoniae* and its role as a human pathogen. Clin. Microbiol. Rev. 17, 697–728.

53. Waller, J.L., Diaz, M.H., Petrone, B.L., Benitez, A.J., Wolff, B.J., Edison, L., Tobin-D'Angelo, M., Moore, A., Martyn, A., Dishman, H., Drenzek, C.L., Turner, K., Hicks, L.A., Winchell, J.M., 2014. Detection and characterization of *Mycoplasma pneumoniae* during an outbreak of respiratory illness at a university. J. Clin. Microbiol. 52,849–853.

54. Wawegama, N.K., Markham, P.F., Elso, C.M., Kanci, A., Marenda, M.S., Browning, G.F., Brodnicki, T.C., 2018. Autoimmune-disease-prone NOD mice help to reveal a new genetic locus for reducing pulmonary disease caused by *Mycoplasma pulmonis*. Infect. Immun. 86, e00812–17.
55. Wilson, K.R., Napper, J.M., Denvir, J., Sollars, V.E., Yu, H.D., 2007. Defect in early lung defense against *Pseudomonas aeruginosa* in DBA/2 mice is associated with acute inflammatory lung injury and reduced bactericidal activity in naïve macrophages. Microbiology 153, 968–979.
56. Wonnenberg, B., Jungnickel, C., Honecker, A., Wolf, L., Voss, M., Bischoff, M., Tschernig, T., Herr, C., Bals, R., Beisswenger, C., 2016. IL-17A attracts inflammatory cells in murine lung infection with *P. aeruginosa*. Innate Immun. 22, 620–625.

ACKNOWLEDGEMENTS

First and foremost, I would like to express my sincere gratitude to my supervisor Prof. Takashi Agui (Graduate School of Veterinary Medicine, Hokkaido University), for giving me the opportunity to study in the Laboratory of Laboratory Animal Science and Medicine, Hokkaido University, also his continuous support during my Ph.D. study and related research, for his patience, motivation and immense knowledge. His guidance helped me at all the time of research and writing of this dissertation.

Besides my supervisor, I would like to express my deepest appreciation to Assoc. Prof. Masami Morimatsu (Graduate School of Veterinary Medicine, Hokkaido University), and Assist. Prof. Hassan Tag EL-Din (Graduate School of Veterinary Medicine, Hokkaido University) for his continuous helps and encouragement in research experiments with critical comments to improve the study outline and activities.

Furthermore, I would like to thank the member of my thesis committee; Prof. Kazuhiko Ohashi (Graduate School of Veterinary Medicine, Hokkaido University), Assoc. Prof. Satoru Konnai (Graduate School of Veterinary Medicine, Hokkaido University), and Assoc. Prof. Yuko Okamatsu (Graduate School of Veterinary Medicine, Hokkaido University), for their insightful comments and encouragement.

My gratitude also extends to Dr. Nobuhito Hayashimoto (Central Institute for Experimental Animals, Japan), Assoc. Prof. Norikazu Isoda (Research Center for Zoonosis Control, Hokkaido University), and Dr. Akio Suzuki (Faculty of Veterinary Medicine, Hokkaido University) for their constant support and assistance. I am also thankful to all laboratory members for helping me during my experiments and sharing every unforgettable moment.

Additionally, I would like to express my sincere gratefulness to Prof. Motohiro Horiuchi (Dean of Graduate School of Veterinary Medicine, Hokkaido University) and all staffs of academic affairs section, leading program office (Specially Ms. Maki and Ms. Terashima), Ministry of Education, Culture, Sports, Science and Technology (MEXT) and to all who supported throughout my Ph.D. course.

Finally, I must express my very profound gratitude to my parents (Mr. Tossaporn and Mrs. Tussana Boonyarattanasoonthorn), family, and close friends for providing me with unfailing support and continuous encouragement throughout my years of study and through the process of researching and writing this dissertation. This accomplishment would not have been possible without all these people.

Thank you.

SUMMARY IN JAPANESE

マイコプラズマ感染は呼吸器に障害を与え非定型肺炎を引き起こすため、世界中でヒト及び動物に対し深刻な問題を与えている。マイコプラズマのうち、とりわけ *Mycoplasma pulmonis* (*M. pulmonis*)はげっ歯類に肺炎を引き起こすため、特定病原体フリーのげっ歯類の微生物学的試験の対象病原体として重要である。それ故 *M. pulmonis* はげっ歯類を用いる研究にとって重大な脅威となっている。複数のマウス系統を用いた先行研究において、この病原体の感染に対し各系統は異なる感受性を示すことが示された。例えば、C57BL/6 (B6)マウスは DBA/2 (D2) マウスに比べ肺に存在する菌体数が 10 万分の 1 で、更に肺のマクロ病変及び組織学的病変が少ないことが知られている。しかし、この感染抵抗性/感受性を規定している細胞免疫反応のプロファイリングと責任遺伝子座あるいは責任遺伝子については殆ど調べられていない。

第一章では、これら 2 系統のマウスにおいて、肺の組織病理学的病変、肺における菌の増殖、肺浸潤細胞、気管支肺胞洗浄液中のサイトカイン、及び縦隔脂肪組織中のリンパ球集団を調べることで、*M. pulmonis* 感染に対する細胞免疫反応を調べた。D2 マウスは B6 マウスに比べて、肺における *M. pulmonis* の高いコロニー形成率、肺のより重篤な病変、より多くの肺への免疫細胞の浸潤、より高いレベルの気管支肺胞洗浄液中のサイトカインなどが見られた。本研究によって初めて B6 マウスと D2 マウスの間でこのような細胞免疫反応に違いがあることが調べられた。これらの結果は D2 マウスでは過剰免疫炎症反応が起こることによって、B6 マウスに比べて *M. pulmonis* 感染に対してより感受性となることを示唆している。

第二章では、B6 マウスと D2 マウスの違いを規定している遺伝因子を明らかにする目的から、第一章で示された量的フェノタイプ（QT）を用いて QTL（quantitative trait locus）解析を行った。それぞれのフェノタイプで検出された QTL はそれぞれ違っていた。このことは、B6 マ

ウスと D2 マウス間で見られるフェノタイプの違いはそれぞれ別の遺伝因子で規定されていることを示唆している。しかし、感染後の体重減少率を QT とした時に、唯一有意な QTL を第 4 染色体に検出することができた。この QTL のピークは *D4Mit42* 座位、151.6 Mbp に位置しており、3.6 LOD スコアを示していた。この座位は第 4 染色体の遠位端に位置し、*D4Mit54* と *D4Mit256* 座位の間で、17.1 Mbp の距離を有していた。この部位に *M. pulmonis* 感染に関与すると思われるいくつかの候補遺伝子が存在した。この座位の更なる研究によりマウスのマイコプラズマ感染症の治療方法に関する知見がもたらされることが期待される。

結論として、この研究から B6 マウスと D2 マウスにおける *M. pulmonis* 感染に対する細胞免疫反応の全体像が明らかにされた。これらのデータは *M. pulmonis* 感染に対する免疫システムの理解を向上させ、*M. pulmonis* 感染に対する宿主免疫反応に関与する遺伝子の同定に貢献するであろう。更にこれらの結果はヒトを含む他の動物のマイコプラズマ症に外挿できるであろう。